NASA TECHNICAL NOTE

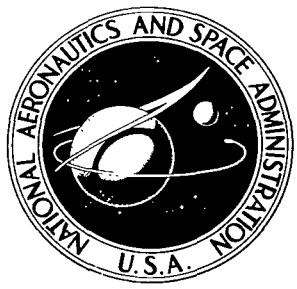

NASA TN D-6115

DESIGN OF THE 20-MEGAWATT LINEAR PLASMA ACCELERATOR FACILITY

by Arlen F. Carter, Willard R. Weaver, Donald R. McFarland, Stephen K. Park, and George P. Wood

Langley Research Center
Hampton, Va. 23365

NATIONAL AERONAUTICS AND SPACE ADMINISTRATION • WASHINGTON, D. C. • JANUARY 1971

1. Report No.	2. Government Accession No.	3. Recipient's Catalog No.
NASA TN D-6115		

4. Title and Subtitle	5. Report Date
DESIGN OF THE 20-MEGAWATT LINEAR PLASMA ACCELERATOR FACILITY	January 1971
	6. Performing Organization Code

7. Author(s)	8. Performing Organization Report No.
Arlen F. Carter, Willard R. Weaver, Donald R. McFarland, Stephen K. Park, and George P. Wood	L-7405
	10. Work Unit No. 129-02-22-04
9. Performing Organization Name and Address	11. Contract or Grant No.
NASA Langley Research Center Hampton, Va. 23365	
	13. Type of Report and Period Covered
12. Sponsoring Agency Name and Address	Technical Note
National Aeronautics and Space Administration Washington, D.C. 20546	14. Sponsoring Agency Code

15. Supplementary Notes

16. Abstract

The design of the 20-megawatt linear plasma accelerator facility at the Langley Research Center – a linear, steady-flow, Faraday-type plasma accelerator for high-velocity aerodynamic testing and basic research in magnetohydrodynamics – is described. Discussion is included on the general design philosophy that leads to three design criteria: (1) make the vector product of current density and magnetic flux density as large as practicable, (2) operate with approximately constant current density, and (3) maintain the Hall potential gradient constant across and along the channel. Use was made of experience and results obtained with previous smaller, lower velocity accelerators. The design exit velocity is 13 km/sec at a density that corresponds to an altitude of 53 km. Many aspects of the engineering design of the accelerator and auxiliary equipment are discussed.

17. Key Words (Suggested by Author(s))	18. Distribution Statement
Magnetohydrodynamics High-enthalpy, high-density flow Faraday accelerator Plasma accelerator design	Unclassified – Unlimited

19. Security Classif. (of this report)	20. Security Classif. (of this page)	21. No. of Pages	22. Price*
Unclassified	Unclassified	53	$3.00

*For sale by the National Technical Information Service, Springfield, Virginia 22151

DESIGN OF THE 20-MEGAWATT LINEAR PLASMA ACCELERATOR FACILITY

By Arlen F. Carter, Willard R. Weaver, Donald R. McFarland,
Stephen K. Park, and George P. Wood
Langley Research Center

SUMMARY

The design of the 20-megawatt linear plasma accelerator facility at the Langley Research Center – a steady-flow, Faraday-type plasma accelerator for high-velocity aerodynamic testing and basic research in magnetohydrodynamics – is described. Use was made of experience and results obtained with previous smaller, lower velocity accelerators. The design was based on three general criteria: (1) make the vector product of current density and magnetic flux density as large as practicable, (2) operate with approximately constant current density, and (3) maintain the Hall potential gradient constant across and along the channel. The latter two criteria were not strictly adhered to over a small upstream portion of the accelerator channel because of a modification to the distribution of accelerator magnetic flux density to avoid improper operation of the arc-heater plasma source and to avoid difficulties with the supersonic nozzle. This modification was considered necessary and was not expected to affect the flow uniformity of the gas at the accelerator exit.

The equations describing accelerator performance were numerically integrated and accelerator operating parameters were obtained. The design exit velocity of the nitrogen plasma was 13 km/sec at a density that corresponds to an altitude of 53 km. It was determined that a cesium concentration of 2 percent mole fraction (based on molecular nitrogen) was required to match properly the voltage required by the accelerator to the voltage available from an existing power supply.

The channel design was accomplished by the use of boron nitride, beryllium oxide, and copper. Cooling was effected by nucleate-boiling heat transfer and the coolant was deionized water. A unique sandwich-like channel construction that used the accelerator electrode insulators as gaskets eliminated the need for mounting the accelerator in a vacuum tank.

The arc heater is described in detail and the design details of the supersonic nozzle necessary to obtain desired accelerator entrance conditions are delineated. Also described are the cesium seeding system, magnet, accelerator resistor network, test section, exhaust system, and facility instrumentation as well as the practical engineering considerations necessary to effect their design.

INTRODUCTION

The Langley Research Center has been engaged in a program to develop a linear, steady-flow, Faraday-type plasma accelerator facility for high-velocity aerodynamic testing and basic research in magnetohydrodynamics. In March 1961 the first positive evidence of steady-state acceleration of a high-density plasma was reported (ref. 1). The accelerator had a channel so small, 10 mm by 10 mm, that diagnostic measurements were limited (refs. 2 and 3). A larger unit, the one-inch-square plasma accelerator at the Langley Research Center, that incorporated a channel 25.4 mm by 25.4 mm composed of 24 electrode pairs was then designed and built. This unit was intended to serve as a pilot model for another much larger accelerator. The device worked well; it accelerated a nitrogen plasma from 2 km/sec to 6 km/sec in a length of 0.3 m (refs. 4, 5, and 6). With the knowledge gained from this previous experimental work and from associated theoretical studies, a larger, higher velocity accelerator, the 20-megawatt linear plasma accelerator facility at the Langley Research Center, has been designed. The design was based on the achievement of an exit velocity of approximately 13 km/sec at a density that corresponds to an altitude of 53 km. This velocity and this altitude were in the range of interest for earth reentry from some other members of the solar system (e.g., ref. 7). The design of the facility is described, discussed, and explained in detail in the present paper.

The facility has been constructed, and has had limited operation. Some experimental results and operating experiences with various components and with the facility as a whole have been obtained. These will be described in a subsequent paper.

SYMBOLS

a	speed of sound, m/sec
A	cross-sectional area, m^2
$\vec{B}$	magnetic flux density, T
c_p	specific heat at constant pressure, J/kg-K
D	hydraulic diameter, $\frac{\text{Four times area}}{\text{Circumference}}$, m
e	elementary charge, C
$\vec{E}$	electric field strength, V/m
f	friction factor, dimensionless

h enthalpy, J/kg

$\vec{j}$ current density, A/m^2

l distance across accelerator channel perpendicular to $\vec{B}$, m

$\dot{m}$ mass-flow rate, kg/sec

M Mach number, u/a

m_N mass per kilogram mole of atomic nitrogen, kg/kmole

n number density, m^{-3}

p pressure, N/m^2

q heat-transfer rate from gas per unit wall area, W/m^2

$R = \frac{R_o}{2m_N}$, J/kg-K

R_o universal gas constant, 8314 J/kmole-K

T temperature, K

$\vec{u}$ velocity, m/sec

$\vec{V}$ potential difference, V

w electrode width in axial (flow) direction, m

x distance in axial (flow) direction, m

y distance in direction of applied electric field, m

z distance in direction of magnetic field, m

Z departure coefficient, $\frac{p}{\rho RT}$

$\beta \equiv \frac{\gamma ZR(1 + \lambda)}{c_p}$, dimensionless

$\gamma \equiv \left(\frac{\partial \ln p}{\partial \ln \rho}\right)_s$

$\lambda \equiv \frac{T}{Z}\left(\frac{\partial Z}{\partial T}\right)_p$

μ coefficient of viscosity, kg/m-sec

$\nu \equiv -\frac{p}{Z}\left(\frac{\partial Z}{\partial p}\right)_T$

ρ mass density, kg/m^3

σ scalar electrical conductivity, mho/m

σ_{eff} effective electrical conductivity in direction of applied $\vec{E}$, mho/m

τ mean free time, sec

ω cyclotron frequency, sec^{-1}

Subscripts:

e electron

p pressure

s entropy

T temperature

x component in x-direction

y component in y-direction

z component in z-direction

Magnitudes of vector quantities are denoted by the same symbol without the arrow.

DESIGN PHILOSOPHY

The approach of this paper to the design of a plasma accelerator begins with a consideration of the equations describing accelerator performance. The equations were developed in references 5, 8, and 9 for a nonperfect gas and quasi-one-dimensional flow. As indicated in figure 1, the only components of velocity and magnetic flux density considered were u_x and B_z. The Hall effect was included, and therefore both E_x and E_y components of the electric field were significant. It is important to note, however, that the one-dimensional analysis considers all these components, as well as the temperature, pressure, density, conductivity, and so forth, to be uniform over the channel cross section. The magnetic Reynolds number was small enough (less than unity) for Maxwell's equations to be considered uncoupled from the fluid equations; the heating due to ion slip was calculated by the method of reference 9 and was found to be negligibly small; and the gas was assumed to be in thermodynamic equilibrium. In reference 5, the real-gas effects caused the conventional $(M^2 - 1)$ coefficient to be replaced by a more complex term and in reference 6 it was shown that all real-gas effects could be included in one quantity β, and thus the equations were returned to the more familiar form. In this latter form it was evident that no real-gas effects explicitly modified the velocity dependence on the $\vec{j} \times \vec{B}$ Lorentz force term. The equations, as derived in reference 6, are

$$\frac{M^2 - 1}{M^2}\frac{du}{u} = \frac{jB}{\rho u^2}dx - \beta\left(\frac{j^2}{\sigma} - \frac{4q}{D}\right)\frac{dx}{\rho u^3} - 2f(\beta + 1)\frac{dx}{D} + \frac{1}{M^2}\frac{dA}{A} \tag{1}$$

$$\left(\frac{M^2 - 1}{\beta M^2}\right)\frac{dT}{T} = -\frac{jB}{\rho u^2}dx - \frac{dA}{A} + \left(\beta M^2 + \frac{M^2 - 1}{1 + \lambda}\right)\left(\frac{j^2}{\sigma} - \frac{4q}{D}\right)\frac{dx}{\rho u^3} + 2f\left(\beta M^2 + 1 + \frac{M^2 - 1}{1 + \lambda}\right)\frac{dx}{D} \tag{2}$$

$$\left(\frac{M^2 - 1}{M^2}\right)\frac{d\rho}{\rho} = -\frac{jB}{\rho u^2}dx - \frac{dA}{A} + \beta\left(\frac{j^2}{\sigma} - \frac{4q}{D}\right)\frac{dx}{\rho u^3} + 2f(\beta + 1)\frac{dx}{D} \tag{3}$$

$$\left(\frac{M^2 - 1}{\gamma M^2}\right)\frac{dp}{p} = -\frac{jB}{\rho u^2}dx - \frac{dA}{A} + \beta M^2\left(\frac{j^2}{\sigma} - \frac{4q}{D}\right)\frac{dx}{\rho u^3} + 2f\left(\beta M^2 + 1\right)\frac{dx}{D} \tag{4}$$

$$\left(\frac{M^2 - 1}{M^2}\right)\frac{d(\gamma M^2)}{\gamma M^2} = (\gamma + 1)\frac{jB}{\rho u^2}\,dx + \frac{\gamma M^2 - M^2 + 2}{M^2}\,\frac{dA}{A}$$

$$- \beta\left(\gamma M^2 + 1\right)\left(\frac{j^2}{\sigma} - \frac{4q}{D}\right)\frac{dx}{\rho u^3} - 2f\left[\gamma + 1 + \beta\left(\gamma M^2 + 1\right)\right]\frac{dx}{D} \tag{5}$$

$$\left(M^2 - 1\right)\frac{dh}{u^2} = -\frac{jB}{\rho u^2}\,dx + \left(\beta M^2 + M^2 - 1\right)\left(\frac{j^2}{\sigma} - \frac{4q}{D}\right)\frac{dx}{\rho u^3} - \frac{dA}{A} + 2fM^2(\beta + 1)\frac{dx}{D} \tag{6}$$

where

$$\beta \equiv \frac{\gamma ZR(1 + \lambda)}{c_p} \tag{7}$$

and

$$\gamma \equiv \left(\frac{\partial \ln p}{\partial \ln \rho}\right)_s = \frac{c_p}{c_p(1 + \nu) - (1 + \lambda)^2 RZ} \tag{8}$$

Investigation of the equations and previous experience with smaller accelerators (refs. 1 to 6) have resulted in a basic philosophy for accelerator design which can be stated as follows:

(1) The $\vec{j} \times \vec{B}$ Lorentz force should be as large as practicable. The $\vec{j} \times \vec{B}$ term dominates the velocity equation, even for moderate values of j and B, and the greater its magnitude, the shorter the accelerator for a given exit velocity. Therefore, j and B should be as large as practicable; however, each will be limited: j by the erosion rate of the insulators or the electrodes and B by practical engineering considerations in the magnet design.

(2) The current density j should be approximately constant. If j is limited by erosion, then the maximum permissible value should be maintained throughout the channel to maximize $\vec{j} \times \vec{B}$.

(3) The axial Hall potential difference between electrodes should not exceed the minimum arc-burning voltage for the gas used. From work done with magnetohydrodynamic generators, breakdown along the electrode wall and consequent shorting of the Hall potential was noted for potential differences greater than this (ref. 10). For polyatomic

gases approximately 40 V between adjacent electrodes appears to be a reasonable maximum usable value.

These are general considerations for the practical design of an accelerator. Additional considerations will become apparent in the discussion of later stages of the design.

CHANNEL GEOMETRY

In the design of this accelerator, velocity was taken to be the parameter of prime importance; however, it was not the only consideration. It is desirable to have most of the energy of the flow in directed kinetic energy; therefore, the temperature of the plasma at the accelerator exit should not be significantly greater than at the entrance. A divergent-channel geometry has the twofold advantage that the increasing area aids in the achievement of velocity and acts to cool the gas; however, the divergent-channel geometry does have a significant disadvantage that can best be illustrated by carrying through a sample calculation for the accelerator.

The following parameters were assumed: a current density of 200 kA/m^2, a magnetic flux density of 1.25 T, an effective electrical conductivity of 100 mho/m, and a diverging-channel accelerator approximately 0.5 m in length with a 51- by 51-mm cross section at the entrance and a 102- by 102-mm cross section at the exit. The first and the last electrodes were assumed to be at an axial distance x of 0.034 m and 0.478 m, respectively. This calculation also assumed no heat transfer into or out of the channel, a friction factor of 0.05, and an entrance velocity to the accelerator of 2.65 km/sec. Equations (1) to (6) were numerically integrated to obtain the plasma parameters as a function of accelerator length. The exit velocity was calculated to be 13.4 km/sec, which was in the range of interest.

The important thing to note, however, was the value of the required applied potential difference of the electrodes as a function of accelerator length. If the sheath voltage was neglected, the calculated value of the applied potential difference at the accelerator entrance was 280 V. At the accelerator exit, the large increase in velocity and the increase in channel height resulted in a computed potential difference of 1860 V. When the generated Hall potential difference was added to the applied electrode potential difference, the result was the distribution of anode and cathode potential difference shown in figure 2. Note the very small change in potential difference, approximately 400 V, between the upstream and downstream ends of the anode wall. The increasing voltage required with increasing velocity and channel height, coupled with the fact that the downstream end of the accelerator was more negative than the upstream end because of the Hall potential difference, resulted in an anode potential distribution that was almost constant with length. Along the cathode wall, however, the potential change, approximately

2000 V between the first and the last cathode, was rather large. Thus, the axial Hall potential gradient was not constant across the channel between the anode and cathode walls.

A nonconstant Hall potential gradient is not desirable in the design of an accelerator that is to produce uniform gas flow at the channel exit. This can be understood from two points of view. First, it is the Hall potential gradient which makes it possible for the direction of current flow to be transverse to the direction of fluid flow in a segmented-electrode channel. Large changes in Hall potential gradient over the channel would certainly affect the current distribution between electrodes and result in large values of j_x. An axial component j_x would interact with B_z to give side thrusts, and these forces would be partially balanced by pressure gradients across the channel, which would of course mean gradients of density, temperature, conductivity, and so forth (ref. 11). Second, reference 9 concluded that from the microscopic point of view, the accelerating force on the plasma derives principally from the ions. The ions, moving essentially in the direction of the channel axis and accelerating the neutrals, derive their energy from the Hall potential field. Nonuniformity of the Hall potential gradient would mean nonuniform acceleration of the plasma resulting in nonuniform velocity of the flow from the accelerator exit, an undesirable situation for meaningful use of the flow for testing purposes.

It therefore seemed necessary to specify another design criterion to help insure uniform flow from the accelerator: The Hall potential gradient must be constant over the channel cross section. This could be accomplished only by having the anode and the cathode potential distributions parallel, that is, a constant applied potential difference to all electrodes. To maintain a constant applied potential difference with a divergent channel geometry, B would have to decrease rapidly along the channel length to offset the increase in both u and l in the expression for applied voltage

$$\vec{V} = l\left[\left(\frac{\vec{j}}{\sigma_{eff}}\right) + \left(\vec{u} \times \vec{B}\right)\right]$$

The divergent channel itself would have aggravated the problem of flow velocity uniformity in that crosswise velocity components which would interact with B would have existed in both the y- and z-directions. This interaction would have resulted in a nonuniform velocity distribution over the channel cross section in the yz-plane. Also, the validity of the one-dimensional flow equations depended partly upon whether the channel cross section varied slowly enough.

A convergent channel would likewise have resulted in a nonuniform velocity distribution in addition to having the area-change term of equation (1) work against the achievement of velocity. Furthermore, the fact that the accelerator entrance area would be very large placed rather severe demands on the nozzle and arc-heater design, and the converging walls were not suitable for supersonic flow.

It was apparent therefore that the divergent and convergent channel geometries were not suitable if uniform flow at the accelerator exit was desired. The constant-area channel then was a reasonable choice if B could be tailored successfully to give the required constant applied potential difference.

CONSTANT-AREA DESIGN

The design of a constant-area channel had to be accomplished to match an existing power supply while achieving the desired exit conditions, a velocity of approximately 13 km/sec at a density that corresponds to an altitude of approximately 53 km.

The accelerator electrode walls were segmented to permit the existence of the Hall potential gradient.[1] Preliminary estimates indicated that the number of segments, or electrode pairs, would be much greater than the number of power-supply modules. The power supply had eight separate modules, each rated at 500 V dc at 2500 A. The modules could be connected in any series-parallel combination. Since the number of electrode pairs greatly exceeded the number of power-supply modules, a resistance network was required to divide the current properly among the many electrodes at the proper axial potential gradient.

The disadvantages of a resistance network were many. The distribution of applied potential difference along the anode and cathode walls had to match the distribution of Hall potential difference that is internally generated, or Hall currents, which would degrade accelerator performance, would result. Any change in one of the operating parameters, either intentionally or unintentionally because of channel degradation, for instance, would change the potential match and therefore the performance. The resistance network would be large, would probably require water cooling because of the large amounts of power being dissipated, and would have to be composed of resistors that must be adjustable. With a resistor network, the Hall potential difference generated by the accelerator was limited to some fraction of the output voltage of the power supply, since the difference in potential between the first anode and the last cathode could never exceed the output voltage of the power supply. The Hall potential gradient, given by

$$E_x = \frac{j_y B_z}{n_e e}$$

(ref. 12), indicated that even B, n_e, and j were subject to constraints because of the power supply. These factors are pointed out to show the influence that the power supply had on this design.

---

[1]The Hall mode and cross-connected mode of operation were considered, but the experimental work necessary to prove their feasibility had not been done when this design was undertaken.

Determination of u and B Distributions

Because of the many constraints on the accelerator design, a trial-and-error design procedure was used. The equations that described the accelerator performance were programed with an assumed channel size, a reasonable value of j determined from previous experimental work (refs. 5 and 6), and a constant applied potential difference, and were numerically integrated until the desired exit velocity was achieved. The B distribution was uniquely determined from the relation for applied voltage

$$\vec{V} = l\left[\left(\frac{\vec{j}}{\sigma_{eff}}\right) + \left(\vec{u} \times \vec{B}\right)\right]$$

If j, σ_{eff}, and l were known quantities and if initial conditions at the accelerator entrance were specified for u and B, then the constant value of V was determined, and as u was calculated numerically along the channel length, B was uniquely determined. After the desired exit conditions were achieved, the accelerator had to be matched to the power supply to determine whether sufficient voltage, current, and power were available.

In the interest of clarity, it is believed that the final design should be followed through in detail, rather than describing at length the initial efforts. Where decisions are made, the reasons and justifications for rejection of other alternatives can be given.

The inlet conditions for the accelerator were those values computed as the exit conditions of the nozzle (see table I). It will be shown subsequently in this section that 2 percent mole fraction (based on molecular nitrogen) of cesium seeding was needed to match the voltage required by the accelerator to the voltage available from the power supply. The scalar electrical conductivity of the plasma was calculated to be approximately 800 mho/m (based on 2 percent cesium seeding); the coefficient of viscosity was calculated from reference 13 to be 0.1 g/m-sec; and the dA/A term in equations (1) to (6) was zero for the constant-area channel. The heat loss term 4q/D was also taken to be zero as a simplifying assumption, the justification being that the heat loss occurs primarily from thin boundary-layer regions at the walls. The friction factor f was derived from reference 14 where the Hartmann theory (ref. 15) was improved by taking into account the effect of $\omega_e\tau_e$. The equation for the friction factor is

$$f = \frac{2\sqrt{\mu\sigma}}{\rho u} B\left[\frac{1 + \sqrt{1 + \omega_e{}^2\tau_e{}^2}}{2\left(1 + \omega_e{}^2\tau_e{}^2\right)}\right]^{1/2}$$

and was derived for only the two insulator walls in the channel. However, when it was used for all four walls in the one-inch-square accelerator at the Langley Research Center, good agreement was obtained between the calculated and measured velocities at

the accelerator exit (ref. 6). The calculated value was therefore assumed to apply to all four walls.

With B estimated to be 1.0 T and $\omega_e\tau_e$ estimated to be approximately equal to 10 (ref. 16), f was calculated to be 0.015. The effective electrical conductivity, needed to compute the electrode potential difference, was obtained from the derivation by Hurwitz, Kilb, and Sutton (ref. 17). For values of $\omega\tau >> 1$, the value is given approximately by

$$\sigma_{eff} = \frac{\sigma}{1 + 2\omega_e\tau_e \frac{w}{l}}$$

where σ is the electrical conductivity in the absence of a magnetic field. It was specified that the length l was 63.5 mm, the electrode potential difference V was 650 V, and the current density j was 200 kA/m^2; then the flow parameters were computed.

The velocity distribution is shown in figure 3 and is seen to reach 12.9 km/sec, the range of interest, at an accelerator length of approximately 0.48 m. In this figure and in subsequent figures accelerator parameters are given from the first electrode (0.034 m) to the last electrode (0.478 m) with the accelerator channel entrance taken to be at an axial distance x of zero. The distribution of magnetic flux density is shown in figure 4 where B varies between 2.2 T at the entrance to 0.73 T at the exit; this distribution, however, gave reason for concern.

Modification of B Distribution

Two aspects of the distribution of B prompted further investigation: (1) the effect of the gradient of B on the current density distribution in the accelerator channel and (2) the effect of the large value of B at the accelerator entrance on the performance of the arc heater and nozzle. Estimates of the effect on the current distribution between electrodes of gradients of B approximately equal to those of figure 4 were made and indicated, however, that the current distribution would be only slightly changed from the distribution for constant B. A later theoretical analysis (ref. 18), taking into account the effect of axial gradients of both u and B, confirmed this result.

The large value of B at the first electrode meant that large values of B would also occur at a short distance upstream of the accelerator at the nozzle and, quite possibly, at the arc heater itself. (See dashed portion of initial design distribution of fig. 4.) A large value of B in the nozzle was not desirable, since large currents could possibly be induced by the $\vec{u} \times \vec{B}$ electromotive force. The nozzle was constructed of copper; therefore, any currents induced in the plasma by the flow would be short-circuited, both across the nozzle and in the axial direction. This could reduce the flow velocity and change the velocity or pressure distribution. Furthermore, the effect on the arc heater

of operation in the presence of a high magnetic flux density was not known. The anode was upstream of the nozzle, and the anode spot was made to rotate by a solenoidal field to prevent burnout. If B from the accelerator magnet had been strong in this area, the discharge might have attached to the anode along the field lines, remained stationary, and burned out or severely eroded the anode. Because of the many unknowns associated with a high magnetic flux density in the vicinity of the nozzle and downstream section of the arc heater, a compromise had to be made in the B distribution at the upstream end of the accelerator channel.

Two approaches were taken. First, the accelerator was designed to minimize the gap between the poles of the magnet at the accelerator entrance. The narrower the pole gap, the more rapidly would the fringe field intensity drop as a function of distance. Initial engineering estimates for the accelerator indicated that the minimum gap distance was approximately 140 mm. Second, the peak value of B was lowered until the fringe field reached values considerably below the value of the solenoidal field in the arc-heater anode region.

With a compromise in B, there was some violation of the design criteria of constant applied potential difference, constant j, and constant Hall potential gradient. The computer program had to be altered, for no longer could a constant applied potential difference and a constant j be specified while the u and B distributions were computed. Over the upstream section of the channel, B was specified. The current density would increase to very large values if the 650-V applied potential difference were specified in this region, but j was kept in bounds by specifying that the product jBu was constant and proportional to E_x. Thus, the average E_x was constant and j was limited. When the computed applied potential difference reached 650 V, it was specified as a constant from that point to the end of the channel. The B distribution was then computed as before throughout the rest of the channel. The current density should be somewhat higher than 200 kA/m^2 initially, but should drop rapidly as u increased. When j dropped to 200 kA/m^2, it was specified constant at this value for the rest of the channel length. Four modified distributions of magnetic flux density are shown in figure 4 as curves 1 to 4. Computations were made to determine which of these distributions would result in the least violation of the accelerator design criteria. Distribution 1 was judged to be the most acceptable. A higher peak value for B would have been closer to the design distribution but would have increased B in the vicinity of the arc heater and would have complicated the engineering of the magnet design. A lower peak value would have changed the B distribution over too large a portion of the accelerator channel.

Determination of Accelerator Parameters

The final B distribution (distribution 1) was used in the procedure outlined in the preceding section to compute the accelerator design parameters. The distributions of

magnetic flux density, current density, applied potential difference, pressure, temperature, mass density, and Mach number are shown in figures 5 to 11. The velocity distribution remained the same as in figure 3. The magnetic flux density at the arc-heater anode was reduced to a value lower than the 0.1- to 0.2-T field which rotated the anode spot, and therefore should not significantly influence the arc-heater operation. The magnetic flux density of approximately 1.0 T or less in the vicinity of the nozzle was greater than desired but was not anticipated to cause adverse effects in the nozzle flow. The magnetic flux density in the region of the first few electrodes was approximately 1.3 T, rose to a peak value of 1.43 T approximately 60 mm into the channel, and then dropped to 0.73 T at the last electrode. The current density quickly dropped from 350 kA/m^2 at the first electrode to the desired value of 200 kA/m^2 and then remained approximately constant. The potential difference between electrodes rose quickly from a value of approximately 450 to 650 V, the design value, and then remained constant. The region of higher than average current density and low applied potential difference occurred only over the first 100 mm of the channel. Experience with the one-inch-square accelerator had shown that the applied potential difference across the first several electrode pairs was as much as 150 V higher than the values calculated from the simple one-dimensional theory with end effects neglected. The same computing technique was used for this design; therefore, it was expected that the actual applied potential difference would be greater than the calculated values for the first few electrodes. The low values were thus raised closer to the 650-V desired value. These deviations from the design criteria were not considered significant and helped assure the proper operation of the arc heater and nozzle.

The accelerator design exit conditions are given in table I. The calculated exit velocity of 12.9 km/sec and the density of 0.73 g/m^3 that corresponds to an altitude of approximately 53 km were close to the desired values.

Utilization of Existing Power Supply

The total power requirement into the gas for the accelerator was determined from the preceding section to be 3.8 MW (5800 A total at 650 V). It remained to verify that the voltage required by the accelerator could be matched to the voltage available from the existing power supply. When the calculated Hall potential difference was added to the applied electrode potential differences, the anode and cathode potential distributions shown in figure 12 were obtained. The power supply is shown in this figure divided into four sections with two modules connected in series within each section. It could also be utilized by having each of the eight modules as a single power supply or by having two sections, with four modules connected in series within each section. Of these three modes the most desirable was to have as many isolated supplies as possible because matching the externally applied Hall potential to the internally generated Hall potential

and thereby eliminating the Hall currents could be accomplished much more easily. However, an additional consideration entered into the usage of the power supply modules as single units.

Each module of the power supply was a three-phase, full-wave bridge and had a 360-Hz ripple with an rms amplitude of approximately 4.5 percent of the average voltage output. For a 750-V output, this gave a ripple of 34 V rms, which would have a peak-to-peak value of approximately 96 V. The design applied potential difference of 650 V consisted mostly of back emf, and the applied potential difference responsible for current flow through the resistance of the plasma, the $\frac{j}{\sigma_{eff}} l$ term, had an average value of approximately 85 V. The ripple voltage, then, would have caused a very large alternating component of current through the accelerator, which in turn would have caused the velocity to pulsate at a rate of 360 Hz. (It can easily be shown that the velocity essentially will follow the $\vec{j} \times \vec{B}$ force at this low frequency.) This problem could be reduced, however, if at least two modules were used together.

The power supply was constructed so that two transformers were used to feed the eight modules, four on each transformer. One transformer was Y-Y connected, the other Y-Δ. As a result, there was a phase difference of 30° between the output voltages of the two transformers. The ripple frequency of four modules, being six times the base frequency, therefore was shifted in phase by 180° from the ripple frequency of the other four units. When any module from one group was connected with a module from the other, the effect on the ripple amplitude was the same as converting from three-phase, full-wave to six-phase, full-wave rectification. The ripple factor was reduced from approximately 4 percent to approximately 1 percent. Connecting two modules in series to give four sets to power the accelerator seemed to give the most desirable arrangement.

The voltage available as a function of total current for the three modes of operation can be estimated from figure 13. The total accelerator current was approximately 5800 A, which gave a value of 1280 V for two modules in series. If nine electrodes were used on each section, the maximum potential difference (between the first anode and the last cathode of each section) was obtained by adding the Hall potential difference, 300 V, to the average electrode applied potential difference, 650 V, to give 950 V. The excess voltage was 1280 minus 950 V, or 330 V. It must be remembered that the calculation for electrode potential difference did not include a sheath drop, or "electrode voltage drop." Measurements of sheath voltage made in the one-inch-square accelerator with water-cooled copper electrodes (ref. 6) gave 46 V for the anode and 20 V for the cathode, or 66 V total. Other investigators have observed sheath drops as high as 140 V for a single, highly cooled electrode (ref. 12). Also, some seed material was usually lost by condensation on cold walls in the arc-heater nozzle or in the accelerator; this tended to lower the conductivity and increase the Hall potential difference. Because of these factors it

seemed expedient in this design to retain the excess voltage of 330 V to help assure proper operation of the accelerator. It is apparent then that the existing power supply could be satisfactorily used with the accelerator design based on the conditions listed in table I and those given earlier in this section.

The Hall potential difference of 300 V for each power supply section was computed for 2 percent mole fraction (based on molecular nitrogen) cesium seeding of the nitrogen gas. A smaller percentage than this would reduce the electron concentration, increase the Hall potential gradient, and thereby reduce the excess voltage available. The 2 percent value of seeding was higher than desired, but was necessary for operation within the limitations imposed by the power supply.

ARC HEATER

The arc heater designed to provide the accelerator working gas is shown schematically in figure 14 and consisted of five basic components:[1] cathode, constrictor, transition section, anode, and plenum chamber. Figure 15 is a photograph of the arc heater. The cathode body was a water-cooled brass tube, and 17 percent of the nitrogen working gas was introduced through a 12.7-mm hole on the axis of the cathode. The face was made of a tungsten-base refractory alloy that consisted of 25 percent copper and 75 percent tungsten by weight. The discharge was rotated on the face of the cathode about the axis by a water-cooled coil embedded within the cathode and immediately behind the cathode face. The cathode was mounted within the upstream end of the constrictor section. Sixty-eight percent of the nitrogen was injected tangentially into the constrictor section approximately 51 mm upstream of the face of the cathode.

The constrictor was approximately 1.2 m long and was composed of 61 individually water-cooled segments separated from one another by a boron nitride insulator 1.2 mm thick. A transition section was located immediately downstream of the constrictor. Its purpose was to provide a smooth transition between the 63.5-mm-diameter constrictor section and the 102-mm-diameter anode section. Two percent of the flow was injected immediately upstream of the transition section and 9 percent of the flow immediately downstream. The nitrogen injection in this region as well as in the areas downstream was to prevent electrical breakdown between adjacent electrically isolated components.

The anode was 127 mm long in the axial direction and was fabricated from chromium-copper alloy. The attachment point of the arc was rotated on the anode surface

[1]The description of the components given here was applicable during the months of development and during initial operation of the arc heater. Changes have subsequently been made in the anode, the anode coil, and the configuration of the cathode.

about the flow axis by a magnetic field produced by an external coil. A plenum chamber of the same inside diameter as the anode was located downstream of the anode. Two percent of the nitrogen was injected between the anode and the plenum chamber. Two openings were provided in the plenum chamber into which cesium seeding devices could be inserted. The remaining 2 percent of the flow was injected between the plenum chamber and the supersonic nozzle.

All components of the arc heater were highly cooled with deionized water. All surfaces exposed to the flow were copper or high-strength copper alloy, and all other parts were nonmagnetic stainless steel. The entire arc heater was mounted on a rolling platform so that it could easily be disconnected and rolled back from the accelerator, or with the accelerator removed, rolled forward to mate with the exhaust duct for testing.

NOZZLE

Once the general concept for the accelerator design was formulated, the requirements for the nozzle design became clear. The magnitude of velocity at the accelerator entrance should be as large as practicable, since the lower the velocity, the greater the magnitude of magnetic flux density required for operation with a constant applied electrode potential difference. The problems associated with a large magnetic flux density at the entrance of the accelerator were discussed in the section "Constant-Area Design." Also, the greater the inlet velocity, the smaller would be the change in magnetic flux density through the channel, since an increase in velocity was offset by a decrease in the magnetic flux density to maintain a constant applied electrode potential difference (assuming constant current density). This simplified the design of the magnet and gave better field uniformity. The high velocity had to be achieved by reducing the nozzle minimum area (since the exit area was previously chosen); the arc-heater stagnation pressure was thereby increased for a given enthalpy. The maximum arc-heater operating pressure at a given enthalpy thus determined the nozzle exit velocity and was limited by the state of the art of arc-heater development.

The design mass flow rate was determined by the desired exit conditions of 13 km/sec at a density that corresponds to an altitude of approximately 53 km, or 0.73 g/m^3. For a channel 63.5 mm by 63.5 mm, the mass flow was 36 g/sec. A stagnation enthalpy of 23 MJ/kg was assumed, and from reference 19, a stagnation pressure of 200 kN/m^2 was determined to be within the state of the art for arc heaters. An isentropic equilibrium expansion to Mach 1 with the use of these arc-heater stagnation conditions was computed to determine the cross-sectional area of the nozzle minimum, which was found to be 441 mm^2.

The exit area of the nozzle was fixed, of course, by the accelerator channel dimensions, but the contour of the nozzle needed to be determined to give reasonably uniform flow at the exit. The subsonic contracting section was designed to give a monotonically increasing velocity at the wall and thereby to avoid adverse wall pressure gradients and possible boundary-layer separation (ref. 20). The computer program of reference 21 was used to compute the inviscid contour for the supersonic expanding section. It was believed that a reasonable thermodynamic approximation to the nozzle flow could be obtained by assuming the flow to be in equilibrium in the contracting section and assuming the flow in the expanding section to be nonreacting, with the dissociation percentage frozen at the throat value. Because of the stagnation pressure and enthalpy considered, this approximation was believed to be sufficiently good (ref. 6). Therefore, despite the fact that the computer program of reference 21 was based upon nondissociating nitrogen, it was possible to modify this program to include frozen flow and hence to use it for the expanding section of the nozzle. Reference 21 also stated that to calculate the boundary-layer displacement thickness for stagnation conditions much different from those considered (in ref. 21), considerable modification to that section of the computer program would have to be made. Since these modifications were not considered feasible, only that part of the program which computes the inviscid-flow-field contour was used for the supersonic portion of the nozzle. The boundary layer was then estimated from the Pohlhausen theory, as given in reference 22, and added to the inviscid contour to give the physical nozzle contour. The final nozzle contour is shown in figure 16.

The nozzle-exit velocity, the gas parameter of greatest interest, should be essentially the same whether the gas is frozen or in equilibrium. The computer program for the accelerator calculations was based on thermodynamic equilibrium, which was certainly more realistic than the assumption of frozen flow in the accelerator channel. For consistency then, the computed nozzle-exit velocity and known total enthalpy were used to obtain equilibrium thermodynamic properties to be used as initial inputs for the computer program that described the accelerator performance. The accelerator entrance parameters are listed in table I.

CESIUM SEEDING SYSTEM

The cesium seeding system was a larger version of the apparatus that was used for the one-inch-square accelerator (ref. 5). This apparatus was found to work well, and because of considerable experience with it, no basic change was made in the design. Figure 17 is a photograph of the seeding apparatus. Cesium in a glass vial was inserted into a chamber where it was heated to 322 K to liquefy it. Air was removed by purging the system with nitrogen, the glass vial was broken by a plunger, and the liquid cesium flowed by gravity into a cylinder. A piston driven by a constant-speed motor forced the

liquid cesium into a stainless-steel electrically heated tube that vaporized the liquid metal and injected it into the arc heater perpendicular to the flow axis, downstream of the arc discharge, but upstream of the supersonic nozzle. The chamber that held the cesium vial was made large enough to hold up to 50 g. (The chamber size can easily be increased if necessary.) The design of the tube that vaporized the cesium was the most critical part of the system. The tube diameter had to be large enough to give a small pressure drop due to the vapor flow; the upstream absolute pressure was thereby kept in a region where the boiling point did not become too great. Furthermore, the tube temperature had to be kept above the condensation temperature of the vapor at every point along the tube.

The estimated stagnation pressure in the arc heater at the cesium injection point was approximately 200 kN/m^2. To insure good penetration and mixing of the vapor jet with the nitrogen plasma, the velocity of the cesium should be high, that is, close to sonic velocity. The pressure in the vaporizing tube would then be of the order of 400 kN/m^2. The boiling point of cesium at this pressure was approximately 1110 K (ref. 23). This temperature was low enough that a stainless-steel tube could be used to vaporize the cesium, and the oxidation and mechanical difficulties involved with refractory metal tubing were avoided. A 1.8-m-long tube with an outside diameter of 6.35 mm and a wall thickness of 0.79 mm was found to be very satisfactory. The computed pressure drop, 35 kN/m^2, was small enough that it should not increase the upstream pressure in the tube; therefore, the cesium boiling point would not be increased beyond the temperature capabilities of the tube. The tube could be readily heated to approximately 1150 K by a current of 150 A at 25 V ac. The end of the tube where the vapor was injected into the arc heater presented a problem area in that the tube had to be kept hot to its end to prevent condensation of the cesium vapor but also had to be cooled to prevent melting at the end by radiation and heat conduction from the gas in the arc heater (ref. 5). Because of the small difference between the operating and the melting temperature of the stainless-steel tube, a molybdenum tip was designed and electron-beam-welded to the end of the tube. This gave more temperature latitude to achieve a heat balance. The design of the end of the seeding tube is shown in figure 18. A thermocouple was used to measure the temperature at point b to assure that the temperature of the tip was hot enough to prevent condensation. The length of the molybdenum cylinder from a to b or its radial thickness could be changed to adjust the temperature if necessary.

ENGINEERING DESIGN OF ACCELERATOR

The design problems associated with the successful containment of the high-enthalpy, electrically conducting accelerator gas were many and varied. As is subsequently shown in this section, very high heat-transfer rates to the sidewalls and electrodes of the

accelerator channel were expected. This energy input had to be dissipated to avoid deterioration of the channel walls. The desire for a long test time (several minutes of arc-heater operation and several seconds of accelerator operation) and the expected high thermal flux precluded the use of the channel as a heat sink and required that the channel be constructed of materials with high thermal conductivities and the use of active cooling. At the same time, the sidewalls of the channel and the material between the electrodes had to be good electrical insulators to prevent current flow across the channel through the sidewalls and between adjacent electrodes. This combination of good electrical insulation and good thermal conductivity created a very difficult problem in channel design because of the lack of materials that simultaneously satisfied both criteria. The accelerator also had to be easy to assemble and disassemble and easy to connect to the nozzle at one end and the test section at the other. It also had to be insulated well enough to withstand the Hall potential difference of approximately 1300 V that was developed between the accelerator entrance and exit.

Electrodes

To establish the Hall potential difference, the electrode wall had to be segmented. The number of segments, however, would be determined by the smallest feasible thickness of the electrode. This thickness was found to be approximately 7.9 mm because of cooling requirements and the space requirements of coolant hoses and electrical connections. Boron nitride was selected as the insulator material between electrodes because of its good performance in previous accelerators (refs. 5 and 6), and 4.8 mm was selected for its thickness. From these dimensions and the previously determined length necessary to achieve the desired exit velocity, a total of 36 electrode pairs in the channel were necessary. Since the computed center-line Hall potential difference was 1290 V, the axial potential difference between electrodes was approximately 37 V, which did not exceed the stated design maximum of 40 V between adjacent electrodes.

The energy-transfer rate to an anode was estimated from reference 24 and included both a convective component and a component due to capture of the current-carrying electrons. When this method was applied to the anode heating in the one-inch-square accelerator and exit gas conditions (ref. 5) were used, the total heat-transfer rate to an anode per unit area (the heating was assumed to be uniformly distributed over the anode surface) was found to be approximately 21 MW/m^2. This calculation assumed an estimated sheath voltage drop of 50 V and a current of 65 A. The calculation was considered to be only an estimate, and therefore, several water-cooled copper electrodes were constructed and tested in the one-inch-square accelerator. The measured value of anode heating near the accelerator exit was 21 MW/m^2 at a current level of 65 A (a current density j of approximately 200 kA/m^2). The agreement between the measured and

computed values gave some confidence in the value of sheath voltage, 50 V; the value agreed well with the measurement of sheath voltages at cooled electrodes in reference 12 and was considered reasonable for use in designing the present accelerator. Based on a sheath voltage of 50 V and the design parameters at the exit of the 20-MW accelerator, the estimated anode heat-transfer rate was 29 MW/m^2 at the downstream end.

Because the actual value of the sheath voltage was not known for the one-inch-square accelerator and could not be accurately estimated for the 20-MW accelerator, and because the possibility existed that the design current density for the 20-MW accelerator might be increased, the design heat-transfer rate to an anode in the 20-MW accelerator was taken to be approximately $2\frac{1}{2}$ times the estimate, or 77 MW/m^2. Since this heat-transfer rate was very large, it was decided that from a practical engineering standpoint (reasonable wall temperature and thicknesses, reasonable coolant temperatures and pressures) the cooling should be effected by the nucleate-boiling heat-transfer regime. The water velocity should, therefore, be very high to wipe the vapor away from the surface and to keep the bulk temperature moderate. For a water velocity of 61 m/sec in the electrode passage, the bulk temperature rise was calculated to be less than 11 K. The measured cathode heating rate was found to be approximately one-third that of an anode in the smaller accelerator; therefore, the design anode heating rate should be more than adequate for use in determining cathode cooling requirements.

Sidewalls

The sidewalls of the accelerator presented the problem of designing for high heat-transfer rates combined with the problem of preventing electrical breakdown due to the existence of the large Hall potential gradient developed along the accelerator channel. The channel sidewalls had to provide electrical insulation along the channel as well as across the channel. If water-cooled metal sidewalls were to be used, then they would have to be coated with a dielectric. Reference 6 reported tests that were conducted to determine the most promising type of sidewall construction. Water-cooled copper sidewalls were coated with aluminum oxide and beryllium oxide to determine which type of coating would stand up best to the cesium-seeded plasma. The beryllium oxide coating was superior to the aluminum oxide, but neither coating lasted longer than approximately 10 to 12 sec, accumulated from a series of 3-second tests. The coatings failed from either local melting near the anode wall or from deterioration of the oxide by the cesium. Boron nitride sheets were therefore used to shield the coatings from the flow; the water-cooled copper cooled the boron nitride and reduced erosion. This type of construction appeared to be the most satisfactory and was adopted for the new accelerator.

The heat-transfer rate to the sidewalls of the one-inch-square accelerator was calculated by the method of reference 25 to be 7.6 MW/m^2; the measured value was

3.2 MW/m^2 averaged over the total sidewall area. In this instance the computed value was $2\frac{1}{2}$ times the measured value. The sidewall heating rate in the 20-MW accelerator, based on the design exit conditions, was computed by the same method to be 16 MW/m^2. It was assumed that the computed value overestimated the heating rate by a factor of $2\frac{1}{2}$, as with the smaller accelerator, and since this offered a satisfactory margin for error, the computed value was used as the design condition. Since this heating rate may lead to surface boiling, water velocities were kept high (50 m/sec) and the bulk temperature rise was estimated to be approximately 20 K.

Channel Assembly

The accelerator was designed to operate at a static pressure below 10 kN/m^2 and the accelerator channel had to be sealed from atmospheric pressure. The one-inch-square accelerator was mounted inside a stainless-steel chamber that was connected to the vacuum pumping system (ref. 5). The chamber pressure was adjusted to the static pressure of the flow at the accelerator exit to give shock-free flow. This resulted in a very low differential between the channel and chamber pressures. Thus, the design of the accelerator channel was simplified but electrical breakdown occurred over the outside surfaces of the accelerator at the low pressures (ref. 5). A further difficulty was that the numerous electrical leads and water hoses had to be brought through the walls of the pressure vessel. The alternative to this type of construction was to build a channel of such mechanical integrity that negligible leakage into the channel occurred from atmospheric pressure. Then all external electrical and mechanical connections were easily made without having to go through the walls of a pressure vessel and the ambient pressure of 100 kN/m^2 was high enough to prevent electrical breakdown on the outside of the accelerator. This type of construction was chosen for the present design.

The possibility existed that the boron nitride electrical insulators between the electrodes could be used as gaskets to seal against atmospheric pressure; therefore, a small test assembly was constructed for testing this possibility. The test assembly consisted of alternate rings of brass and 4.75-mm-thick boron nitride and had an outside diameter of 76 mm and an inside diameter of 38 mm. All surfaces were finished to 0.8 μm rms. Five rings of each material were used. The assembly was compressed by bolts between brass plates on each end. The unit was connected to a vacuum system and the leak rate determined for various degrees of compression. The maximum compressive pressure applied was 4.7 MN/m^2 and the measured leak rate was 0.54 μg/m-sec. Based on an estimate of the total length of seal exposed for the accelerator, the estimated leak rate was 0.75 mg/sec. For an accelerator mass flow rate of 36 g/sec, the leak rate was approximately 0.002 percent. This very low leak rate proved the effectiveness of the boron nitride as a sealing gasket, and the accelerator was designed along these lines.

A large copper plate was used at each end of the accelerator to compress the two electrode walls. The compression was supplied by bolting the plates at each end of the two nonconducting, epoxy-laminated fiber-glass bars between the two plates. The boron nitride sidewalls, backed by water-cooled copper, were fitted against each side of the electrodes between the end plates. Nonpriming silicone rubber was used around the sidewall joints for a leak-free seal. It easily peeled off when the unit was disassembled. All tolerances were held to ±25.4 μm for a precise fit and all surfaces were finished to 0.8 μm rms. All copper pieces for the accelerator were oxygen-free, hard copper. To prevent electrical breakdown to the metal, the copper sidewalls and end plates were coated with a 0.5-mm-thick coating of beryllium oxide. Beryllium oxide was used because, when compared with other insulating materials, it possessed the desirable combination of high melting point and superior dielectric strength, and in general, it offered a very durable insulative coating that could be applied to the electrically conductive parts of the accelerator that had to be electrically insulated. The completely assembled accelerator is shown in figure 19.

MAGNET

The desired distribution of magnetic flux density was known (fig. 5) and the minimum gap distance (approximately 140 mm) was determined by the exterior dimensions of the accelerator; it remained to compute the pole geometry necessary to give this flux distribution. The pole geometry was determined by using an unpublished technique developed by Kenneth E. Wakefield of the Plasma Physics Laboratory, Princeton University. The permissible flux nonuniformity was set at 5 percent over the cross section at any location along the 63.5-mm-square channel. An estimate was then made of the pole geometry that would satisfy the design requirements, the three-dimensional distribution of magnetic flux density was computed, and the results were compared with the required values. The estimated pole geometry was then revised in an effort to reduce the regions of greatest disagreement. By this trial-and-error method, the pole geometry was revised until the calculated distribution agreed with the desired center-line values to within approximately 2 percent. This method assumed that the permeability of the pole material being used remained constant; that is, there was no saturation. This assumption was expected to cause some error for magnets designed to operate at high flux densities, as this magnet was, especially in the region at the upstream end of the accelerator where the flux density was maximum. To overcome this problem, the magnet was designed with removable pole caps so that in the event the computed geometry did not give the required flux distribution, minor modifications would be simple, or if necessary, new pole caps could be economically constructed to replace the initial ones. The alternative to this technique would be to build a small-scale model, make measurements of the flux distribution, and adjust the

pole geometry until the proper distribution was obtained. This latter method was not used, however, because the size and the estimated cost of the magnet were of modest proportions.

The final pole geometry with the coils is shown in figure 20. The computed value of 158 000 ampere-turns was supplied by a coil on each side of the gap, each generating 79 000 ampere-turns. The coils were constructed of 7.9-mm-square copper tubing with a 4.3-mm-diameter hole in the center for water cooling. Each coil contained 196 turns of tubing and was designed to operate at 400 A.

RESISTOR NETWORK

A voltage-dividing network had to be utilized to divide the current properly among the many accelerator electrodes. A program was undertaken to develop a resistor capable of satisfying the requirements of adjustability over a suitable range and high power dissipation over a minimum time interval of 10 minutes. This time interval was considered sufficient to include the longest test time that might be attained with the accelerator.

Initial attempts used metal tubing with forced cooling through its interior; however, the entire resistor network would require 72 individual resistors each capable of high power dissipation. To cool such a system properly, a high-velocity coolant at a high flow rate would be required. The necessary pumping equipment to overcome the large pressure losses in such a system was considered too expensive to warrant further consideration in light of other possible alternatives. Since continuous operation was not required it was decided to immerse the resistor material in a static coolant of a large enough volume to absorb the power. Preliminary tests with this concept were undertaken with metal strip that was available locally in short lengths. These strips were welded together and bent into a configuration that could be submerged in a reasonably small container filled with tap water. Several difficulties became immediately apparent. The strip had to be rather thin (less than 1.3 mm thick) or the bending of the strip necessary to get a large length of strip into a container of reasonable size was difficult. Also, wherever short lengths were welded together and wherever sharp bends were made, local overheating of the strip limited its current-carrying capacity.

These initial observations resulted in a working model similar to that shown under construction in figure 21. The strip arrangement is shown for two resistors prior to placement in a container filled with water. The elimination of local overheating of the strip due to bends and welds was accomplished by using one continuous length of metal strip and by folding the strip back on itself in the manner shown in the lower left portion of the figure. A nickel-chromium alloy strip, 9.5 mm by 0.64 mm, was used because of

its availability, ease of forming and handling, high resistivity (1.23 μohm-m at 373 K), low temperature coefficient of resistivity, and high corrosion resistance. The alloy had a nominal chemical composition of 73 percent Ni plus Co, 15.5 percent Cr, 7 percent Fe, 2.5 percent Ti and smaller amounts of C, Mn, S, Si, Cu, Al, Nb, and Ta. Early tests revealed that tap water was undesirable as a coolant because of its high impurity content which resulted in high electrical conductivity and which led to surface scum, deposits, and scale. The ready availability of deionized water (used to cool both accelerator and arc heater) made it the obvious choice of coolant because of its very low impurity level and low electrical conductivity.

A resistor made in this manner was operated at the design condition of 160 A through 9 ohms for 10 min, which corresponds to 260 kW/m^2 of strip surface area. After 3 min steam evolved and after 5 min boiling developed and continued until the 10-min test time was completed. No appreciable loss of water was noted, however, nor was there any indication of local strip overheating. This same configuration was tested at an overload condition of 240 A through 6.3 ohms for 10 min, which corresponds to 580 kW/m^2. The bend in the continuous strip did not overheat but a larger loss of water was noted. Because of this satisfactory performance, testing was terminated. Each final resistor was 9 ohms maximum and was made by folding a continuous strip into 15 lengths approximately 3.0 m long. Five lengths of the strip were mounted one above the other with an epoxy-impregnated fiber-glass insulator separating them and were rigidly clamped to a mounting section of the same material; three of these groups constitute a single resistor. In figure 21 the front three groups of five strips form one resistor and the rear three groups form a second resistor. As presently used, three resistors were immersed in each trough containing 0.60 m^3 of deionized water. The trough was approximately 0.3 m by 0.6 m by 3.4 m and was constructed of glass fiber impregnated with polyester resin.

DEIONIZED-WATER COOLING SYSTEM

Early in the design process, water was chosen as the coolant for the accelerator because it was practical from engineering considerations and was economical. As a primary coolant it eliminated the need for a two-stage system with an intermediate coolant. Two considerations played an important role in the decision that the water should be deionized. First, the very high heat-transfer rates into the accelerator components would almost certainly lead to surface boiling of the coolant. Under these conditions any dissolved material in the coolant would be deposited on the surface and thereby reduce cooling. Previous experience had shown that this scale formation can lead to rapid burnout of the component. Second, it was desirable to minimize electrical losses due to leakage paths through the coolant both between adjacent components and to ground. Deionized water was a coolant that well satisfied these two requirements as it had a

resistivity of approximately 200 kohm-m and an extremely low content of dissolved material. Public supply water was processed through a mixed-bed deionizer containing a strong-acid resin and a strong-base resin. The deionized water produced was stored in a 190 m^3 epoxy-lined storage tank. Stainless-steel piping was used throughout the system to keep dissolved impurities to a minimum. The accelerator pumping system provided 125 kg/sec of water at a pressure of 10 MN/m^2. A separate pump supplied the arc heater with 32 kg/sec of water at a pressure of 5 MN/m^2.

TEST SECTION AND EXHAUST SYSTEM

The downstream end of the accelerator connected to, but was electrically insulated from, a nonmagnetic stainless-steel "test section" attached to the exhaust duct. Its purpose was to provide viewing ports for flow observation and access ports for insertion of various diagnostic probes. Its general appearance can be seen in figure 22. As is shown in this view, the upstream end had to extend between the magnet coils, and the test-section height was severely restricted at this point. The test section had this minimum height for only as short a distance as necessary and then expanded at an 18^o angle to the horizontal to reduce the possibility of flow impingement on the uncooled test section.

The test section was connected to an exhaust duct, 18 m long and 1.5 m in diameter, constructed of high-tensile-strength, corrosion-resistant steel plate rolled and welded into a circular cross section. The diameter of the duct was made large to keep the pressure drop low and to lower the heat-transfer rate for a unit area of wall surface. The duct could then be cooled with an inexpensive low-pressure system using 100 nozzles placed along its length to flood the outside surface of the duct. A flow of 160 kg/sec of water provided an average water velocity over the surface of 1.2 m/sec. The wall thickness of 10 mm was a compromise between making it thick enough to avoid buckling or collapsing and thin enough to keep the inside surface temperature moderate.

The downstream end of the duct connected to a four-stage steam-ejector pumping system. The pumping system, which consumed 3.8 kg/sec of steam at 2.4 MN/m^2, would give no-flow pressure levels as low as 17 N/m^2 and was capable of pumping nitrogen gas at a maximum flow rate of 114 g/sec.

INSTRUMENTATION

As described in reference 5, the large axial potential gradient associated with an earlier accelerator caused considerable inconvenience with that device by finding a circuit external to the plasma through which current could flow: the usual path was to ground and back. The device was plagued by electrical breakdown in recording instruments until these instruments were properly isolated from ground. Based on this previous

experience much effort was expended in isolating all accelerator and arc-heater instrumentation from the recording devices to protect the instruments as well as the personnel monitoring them. Voltage and current measurements were made with transductors that were "dc current transformers," that is, they provided an output current electrically isolated from and proportional to the input.

Two methods were used to record test data. A control room immediately adjacent to the apparatus contained two 36-channel, direct-writing oscillograph recorders to record test data for immediate retrieval. Data also were transmitted to a central data-recording system; test data were converted into direct-current millivolt signals at the test site, carried through underground cables, received at the central recorder, converted into digital form, and stored on tape for later conversion and use with a data-reduction computer program to print out test data in a final form. Two hundred and seventeen channels were available for raw test data, plus 10 channels to designate test number, date, and so forth. The data sample interval was 0.1 sec per channel for each of the 217 channels. Conditions within the room containing the test apparatus were continuously monitored from the control room with three closed-circuit television monitors.

The accelerator system was designed to operate automatically. A typical test sequence proceeded in the following manner. The steam ejector and the exhaust duct, magnet, and accelerator cooling water were turned on manually and set at predetermined levels. The automatic sequence was then initiated, and according to a preset time sequence, the oscillograph recording instrumentation, arc-heater cooling water, seeding-tube heater, and nitrogen flow were automatically activated. Then the arc was powered, cesium flow for seeding was established, and the accelerator was energized. Upon completion of the test, the components were shut down in the reverse order. This type of operation was very advantageous in that it left all personnel available to monitor components and to concentrate on other aspects of the test. All components were interlocked so that if operation occurred above or below preset levels, the automatic sequence would not proceed, a warning was sounded, and a panel indicator which identified the malfunctioning component was activated. The automatic sequence could be terminated manually at any point, or the system could be operated in a completely manual mode.

CONCLUDING REMARKS

The designing of the various components of a high-velocity, high-density plasma accelerator facility has been described in some detail. These components include the arc heater, the cesium seeding system, the supersonic nozzle, the accelerator channel,

the magnet, the resistor network, the test section, the exhaust system, and the instrumentation. Following the designing of the facility as described herein, the facility was constructed and has been put into limited operation. A subsequent paper will describe some operating experiences and experimental results.

Langley Research Center,
National Aeronautics and Space Administration,
Hampton, Va., November 9, 1970.

REFERENCES

1. Wood, George P.: Analysis of Steady-Flow Plasma Accelerator. Bull. Amer. Phys. Soc., ser. II, vol. 6, no. 2, Mar. 20, 1961, pp. 187-188.

2. Wood, George P.; Carter, Arlen F.; Sabol, Alexander P.; and Weinstein, Richard H.: Experiments in Steady-State Crossed-Field Acceleration of Plasma. Phys. Fluids, vol. 4, no. 5, May 1961.

3. Carter, Arlen F.; Wood, George P.; Sabol, Alexander P.; and Weinstein, Richard H.: Experiments in Steady-State High-Density Plasma Acceleration. Engineering Aspects of Magnetohydrodynamics, Clifford Mannal and Norman W. Mather, eds., Columbia Univ. Press, 1962, pp. 45-55.

4. Carter, A. F.; Wood, G. P.; McFarland, D. R.; and Weaver, W. R.: Research on a Linear Direct-Current Plasma Accelerator. AIAA J., vol. 3, no. 6, June 1965, pp. 1040-1045.

5. Wood, G. P.; Carter, A. F.; Sabol, A. P.; McFarland, D. R.; and Weaver, W. R.: Research on Linear Crossed-Field Steady-Flow d.c. Plasma Accelerators at Langley Research Center, NASA. Arc Heaters and MHD Accelerators for Aerodynamic Purposes, Pt. I, AGARDograph 84, Sept. 1964, pp. 1-45.

6. Carter, A. F.; McFarland, D. R.; Weaver, W. R.; Park, S. K.; and Wood, G. P.: Operating Characteristics, Velocity and Pitot Distribution, and Material Evaluation Tests in the Langley One-Inch-Square Plasma Accelerator. AIAA Pap. No. 66-180, Amer. Inst. Aeronaut. Astronaut., Mar. 1966.

7. Bond, Aleck C.; and Faget, Maxime A.: Technologies of Manned Space Systems. Space Flight Technology Series, Enoch J. Durbin, ed., Gorden & Breach Science Publ., c.1965.

8. Wood, George P.; and Carter, Arlen F.: Considerations in the Design of a Steady DC Plasma Accelerator. Dynamics of Conducting Gases, Ali Bulent Cambel and John B. Fenn, eds., Northwestern Univ. Press, c.1960, pp. 201-212.

9. Wood, George P.; Carter, Arlen F.; Lintz, Hubert K.; and Pennington, J. Byron: A Theoretical Treatment of the Steady-Flow, Linear, Crossed-Field, Direct-Current Plasma Accelerator for Inviscid, Adiabatic, Isothermal, Constant-Area Flow. NASA TR R-114, 1961.

10. Brogan, Thomas R.; Powers, William E., Jr.; Liu, Chien; and Mattsson, Arne C. J.: The Application of Matched MHD Generator-Accelerator Units to Hypersonic Wind Tunnel Drive. Presented at AGARD Fluid Dynamics Panel Specialists' Meeting "Arc Heaters and MHD Accelerators for Aerodynamic Purposes" (Rhode-Saint-Genèse, Belgium), Sept. 21-23, 1964.

11. Sutton, George W.; and Sherman, Arthur: Engineering Magnetohydrodynamics. McGraw-Hill Book Co., Inc., c.1965.

12. Louis, J. R.; Lothrop, J.; and Brogan, T. R.: Fluid Dynamic Studies With a Magnetohydrodynamic Generator. Phys. Fluids, vol. 7, no. 3, Mar. 1964, pp. 362-374.

13. Ahtye, Warren F.; and Peng, Tzy-Cheng: Approximation for the Thermodynamic and Transport Properties of High-Temperature Nitrogen With Shock-Tube Applications. NASA TN D-1303, 1962.

14. Fay, James A.: Plasma Boundary Layers. Magnetohydrodynamics, Ali Bulent Cambel, Thomas P. Anderson, and Milton M. Slawsky, eds., Northwestern Univ. Press, c.1962, pp. 337-348.

15. Hartmann, Jul.: Hg-Dynamics I – Theory of the Laminar Flow of an Electrically Conductive Liquid in a Homogeneous Magnetic Field. Kgl. Danske Videnskab. Selskab, Mat.-Fys. Medd., vol. XV, no. 6, 1937.

16. Weber, R. E.; and Tempelmeyer, K. E.: Calculation of the D-C Electrical Conductivity of Equilibrium Nitrogen and Argon Plasma With and Without Alkali Metal Seed. AEDC-TDR-64-119, U.S. Air Force, July 1964.

17. Hurwitz, H., Jr.; Kilb, R. W.; and Sutton, G. W.: Influence of Tensor Conductivity on Current Distribution in a MHD Generator. J. Appl. Phys., vol. 32, no. 2, Feb. 1961, pp. 205-216.

18. Hohl, Frank: Effects of Axial Gradients of Velocity and Magnetic Field, Electrode Stagger, and Ion Slip on Parameters in MHD Accelerators. NASA TN D-4239, 1967.

19. Cann, G. L.; and Harder, R. D.: A Survey and Prediction of the Performance Capability of Coaxial Arc Heaters. Arc Heaters and MHD Accelerators for Aerodynamic Purposes, Pt. I, AGARDograph 84, Sept. 1964, pp. 277-321.

20. Tsien, Hsue-Shen: On the Design of the Contraction Cone for a Wind Tunnel. J. Aero. Sci., vol. 10, no. 2, Feb. 1943, pp. 68-70.

21. Johnson, Charles B.; Boney, Lillian R.; Ellison, James C.; and Erickson, Wayne D.: Real-Gas Effects on Hypersonic Nozzle Contours With a Method of Calculation. NASA TN D-1622, 1963.

22. McAdams, William H.: Heat Transmission. Third ed., McGraw-Hill Book Co., Inc., 1954, p. 224.

23. Heimel, Sheldon: Thermodynamic Properties of Cesium up to 1500° K. NASA TN D-2906, 1965.

24. Lenn, P. D.; Bodoia, J. R.; Ward, D. L.; Hamilton, G. L.; and Demetriades, S. T.: Experimental and Analytical Investigations of Crossed-Field Plasma Accelerators. Part 1. Report of Major Analytic and Experimental Results. ASD-TDR-63-307, U.S. Air Force, May 1963.

25. Moffatt, W. Craig: Boundary Layer Effects in Magnetohydrodynamic Flows. Rep. 61-4 (Contract N-onr-185825), Magnetogasdynamics Lab., Massachusetts Inst. Technol., May 1961.

TABLE I.- DESIGN CONDITIONS FOR 20-MW LINEAR PLASMA ACCELERATOR

Condition	At accelerator entrance (a)	At accelerator exit
Velocity, km/sec	3.8	12.9
Density, g/m^3	2.25	[b]0.73
Temperature, K	5650	8200
Pressure, kN/m^2	5.0	3.3
Enthalpy (stagnation), MJ/kg	23	130
Mach number	2.5	5.5
Mass flow rate (nitrogen), g/sec	36	36
Channel cross-sectional width, mm	63.5	63.5
Channel cross-sectional height, mm	63.5	63.5
Reynolds number per meter		50 000
Stagnation-point heat-transfer rate (based on body diameter of 25.4 mm), MW/m^2		110

[a]Same as nozzle exit conditions.

[b]Equivalent to an altitude of 53 km.

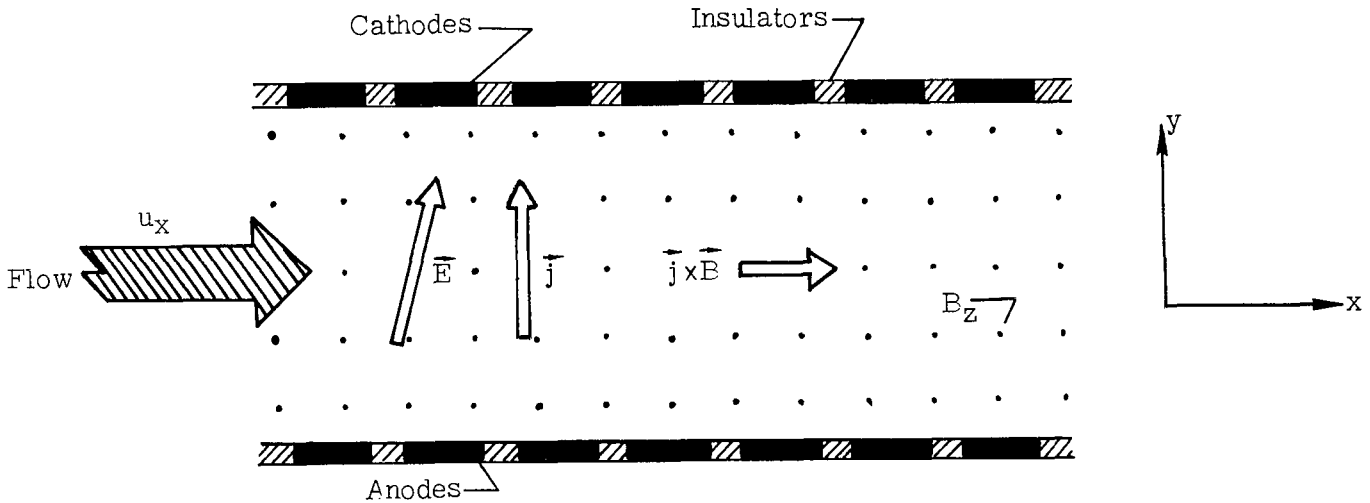

Figure 1.- Schematic diagram of plasma accelerator.

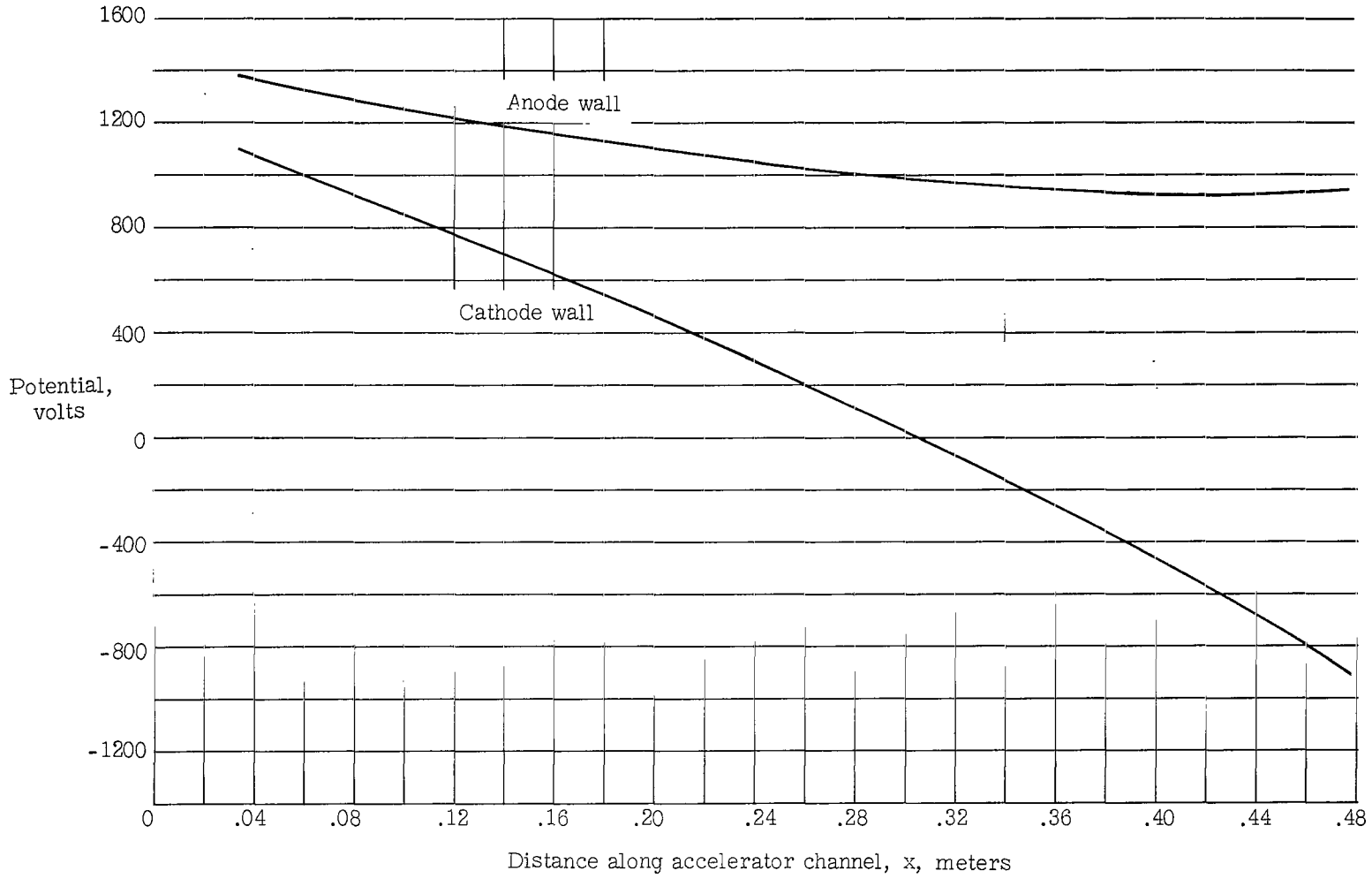

Figure 2.- Potential distribution at anode and cathode walls of a divergent channel.

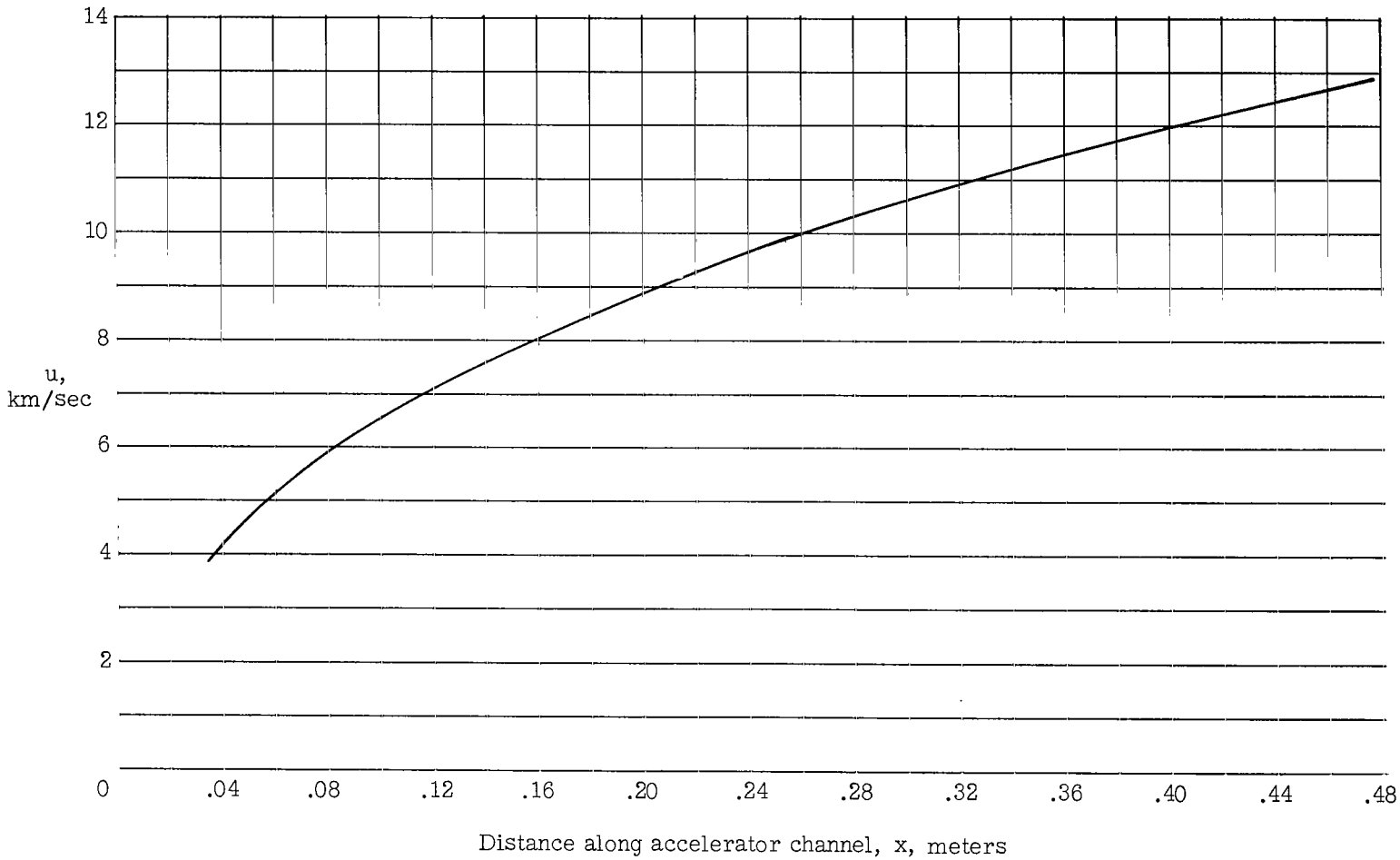

Figure 3.- Velocity distribution.

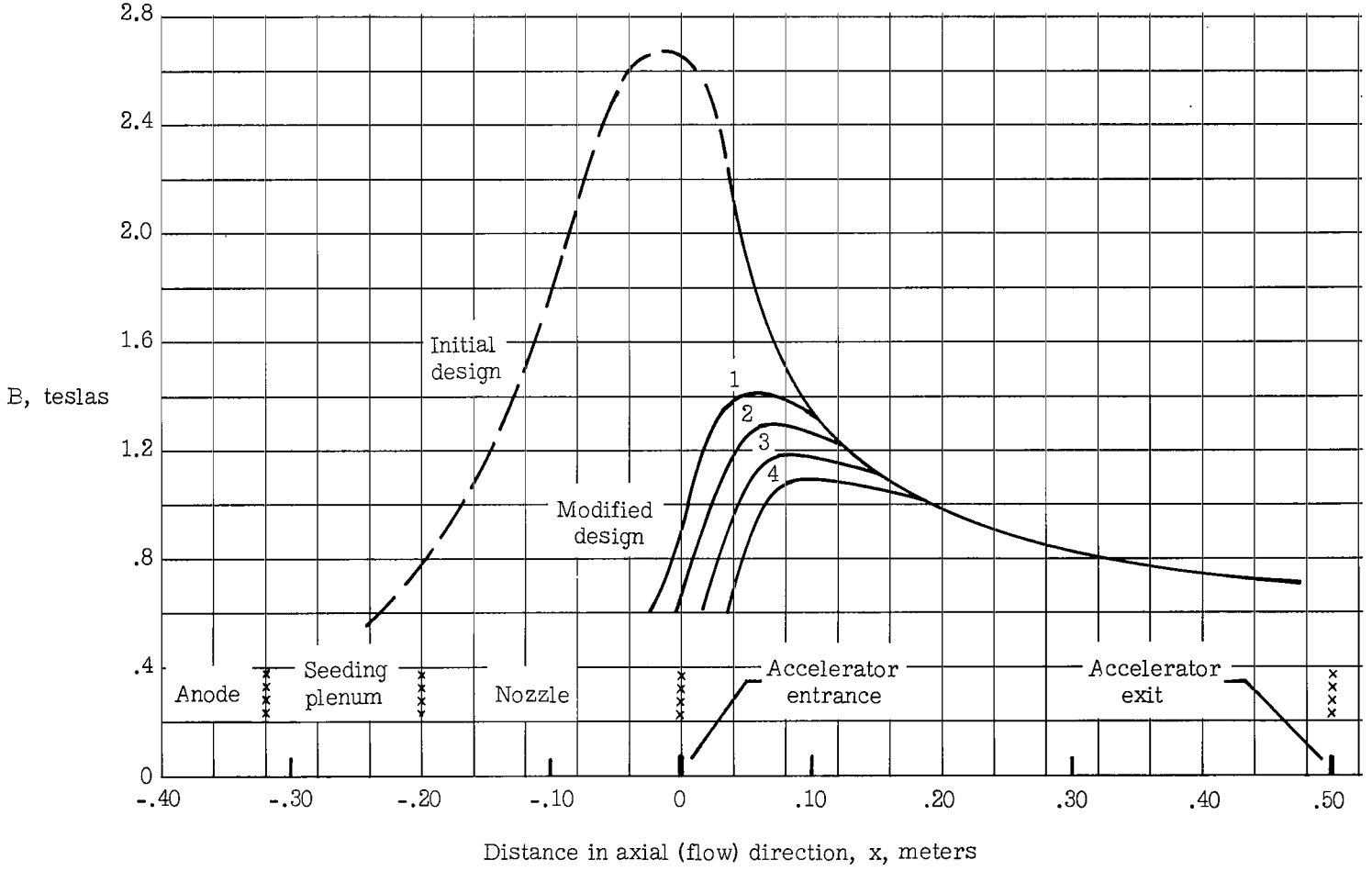

Figure 4.- Alternative distributions of magnetic flux density.

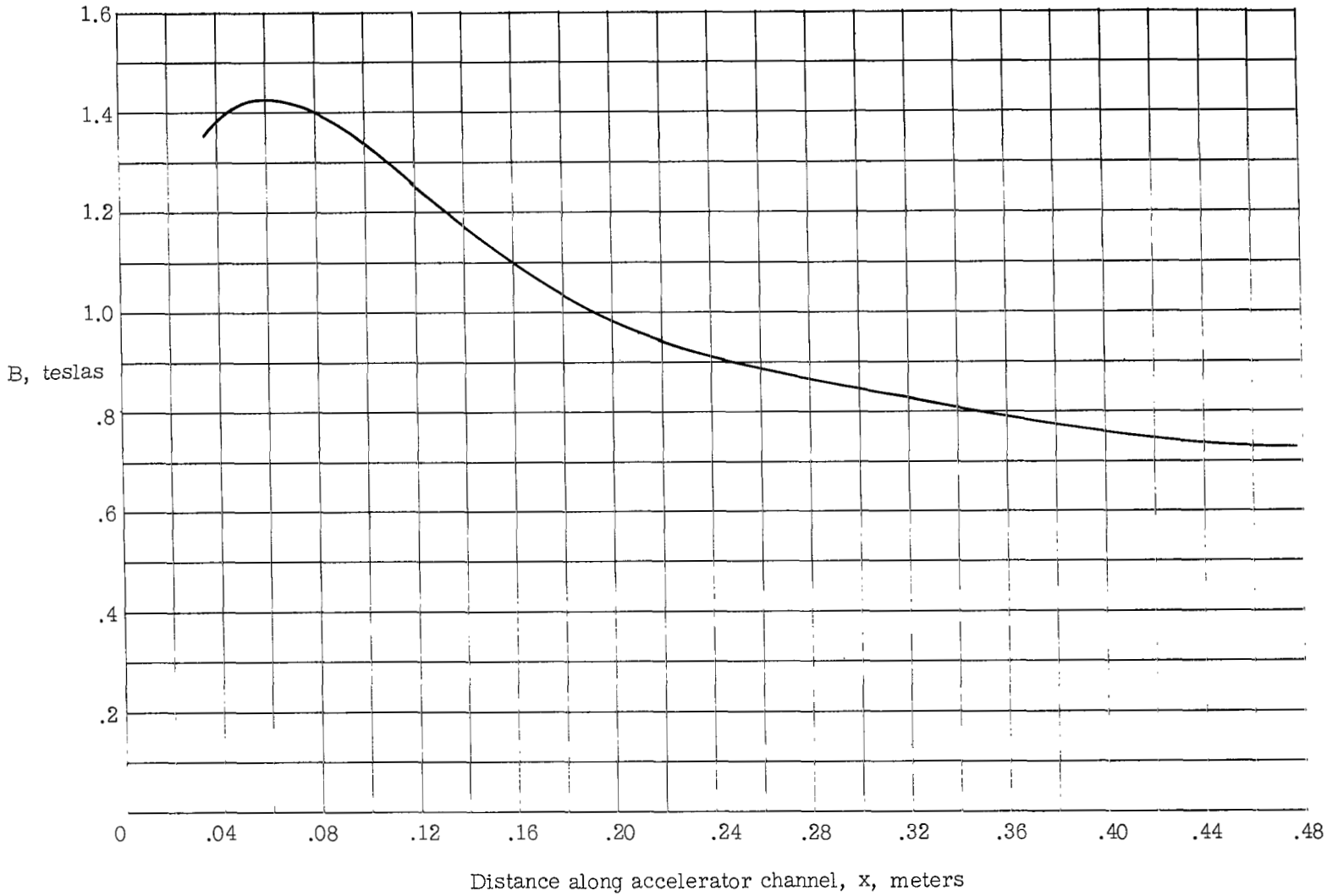

Figure 5.- Final distribution of magnetic flux density.

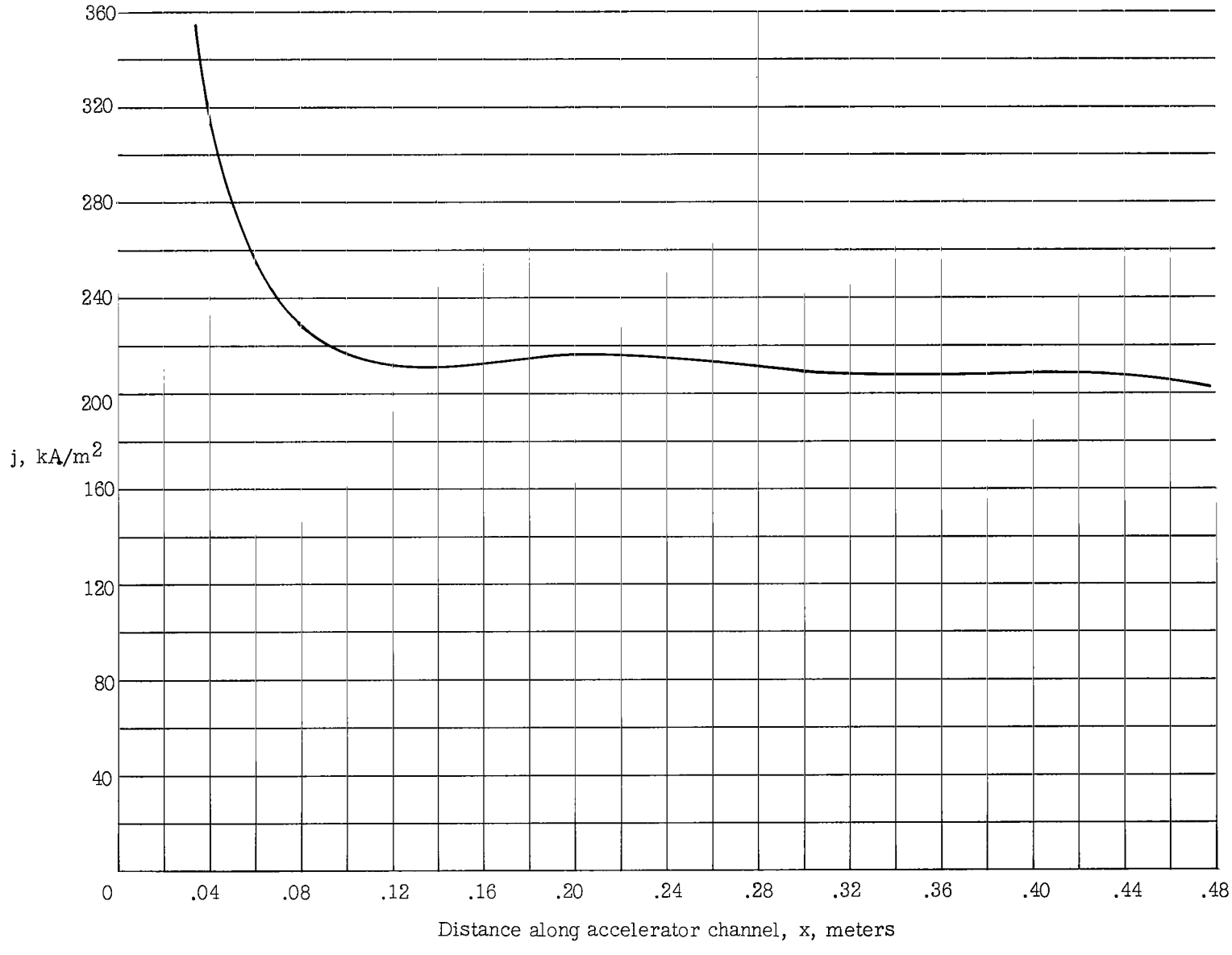

Figure 6.- Current-density distribution along channel center line.

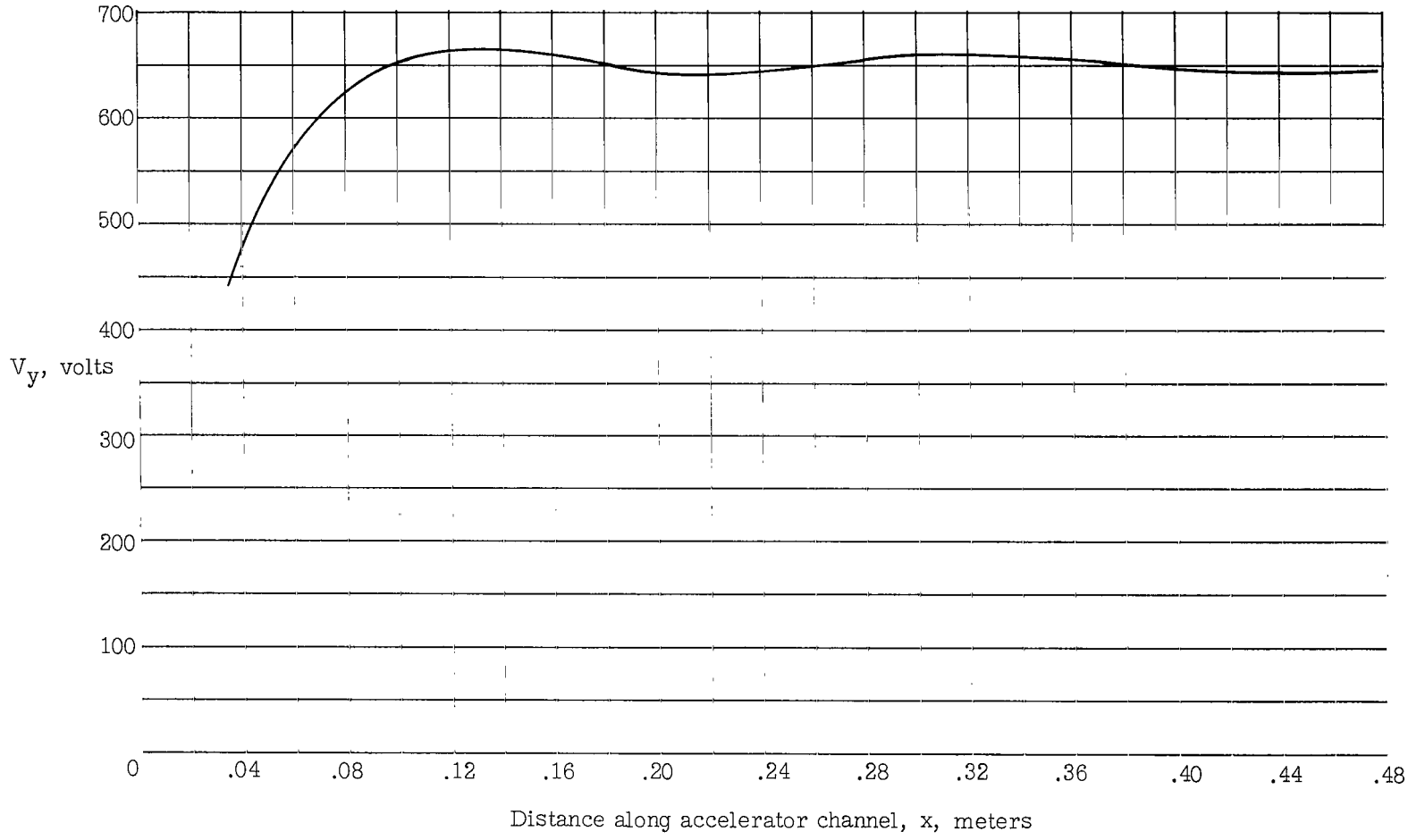

Figure 7.- Distribution of electrode potential difference across the channel.

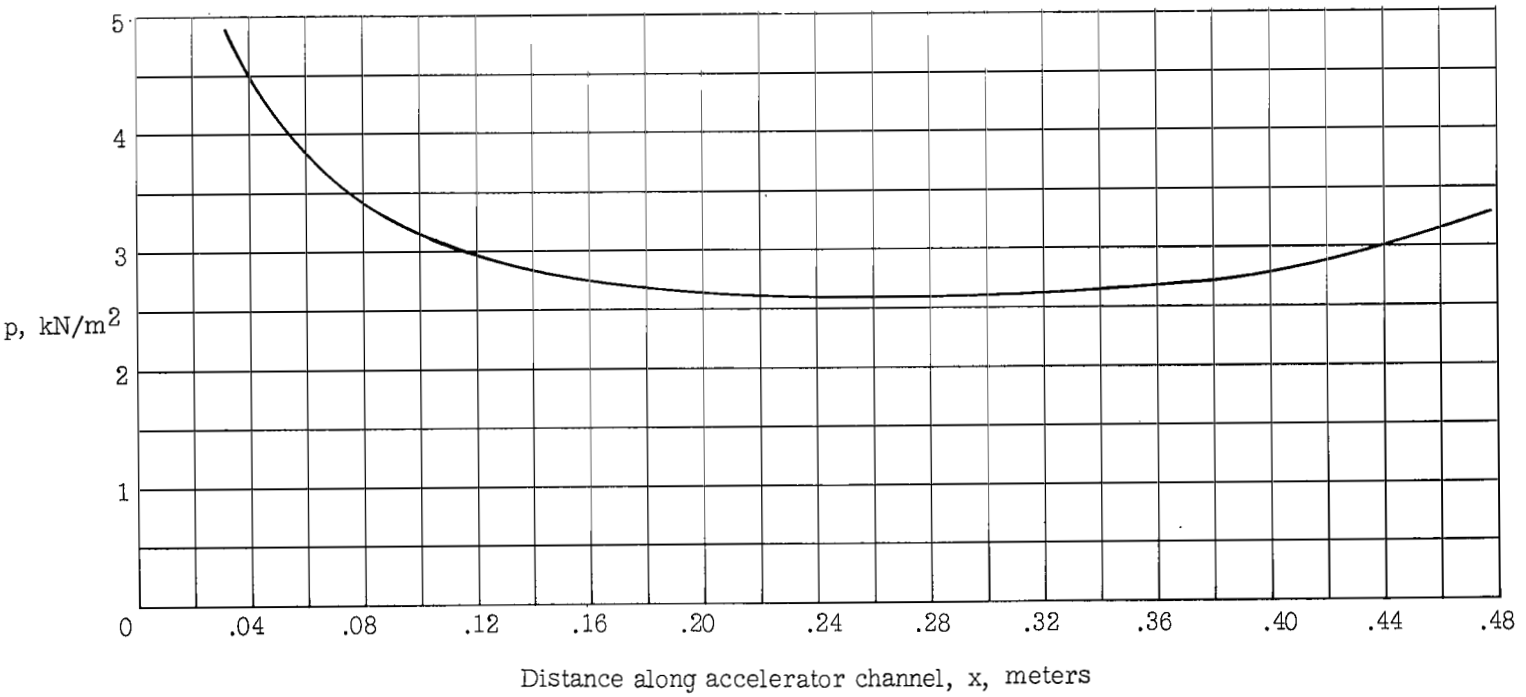

Figure 8.- Static-pressure distribution.

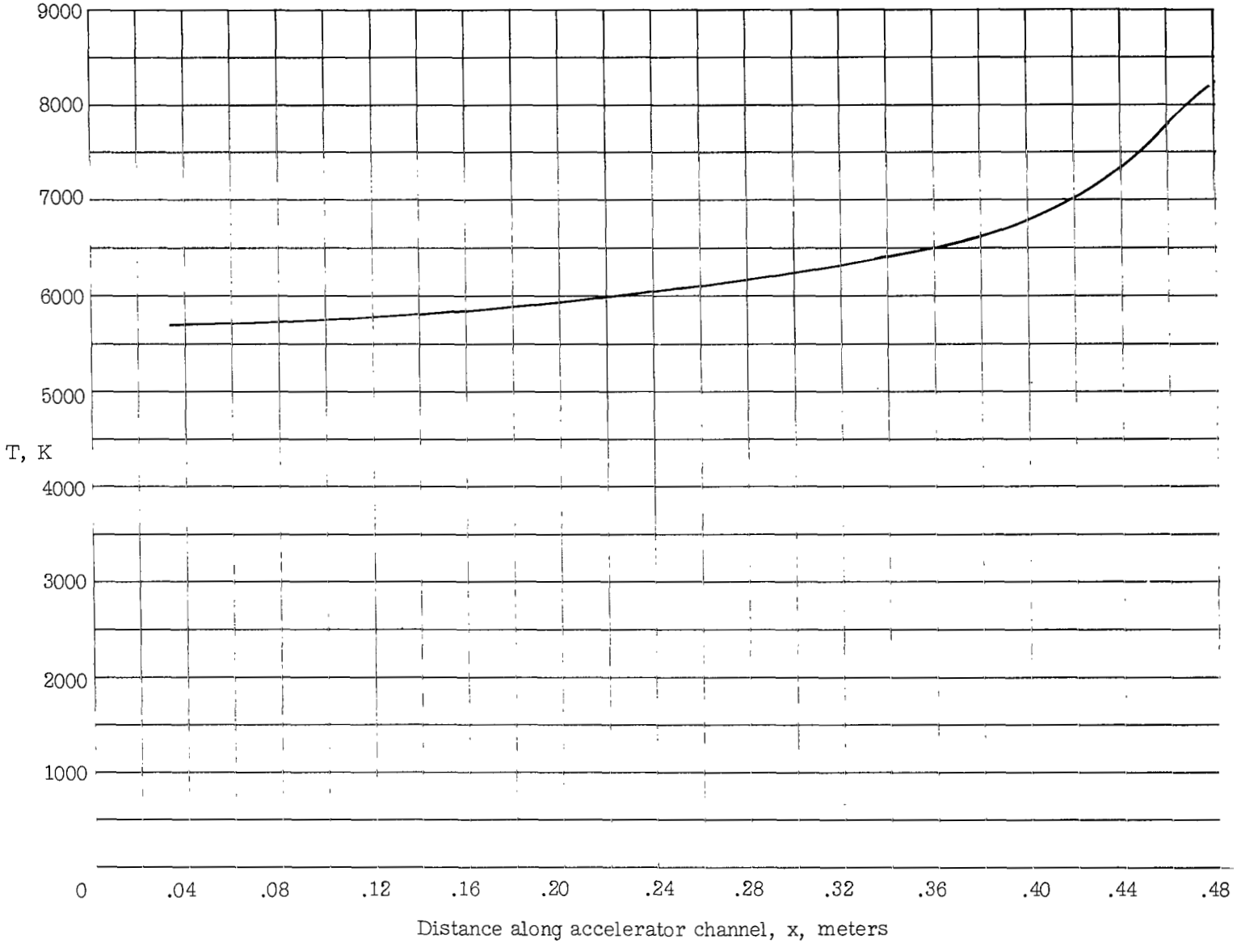

Figure 9.- Static-temperature distribution.

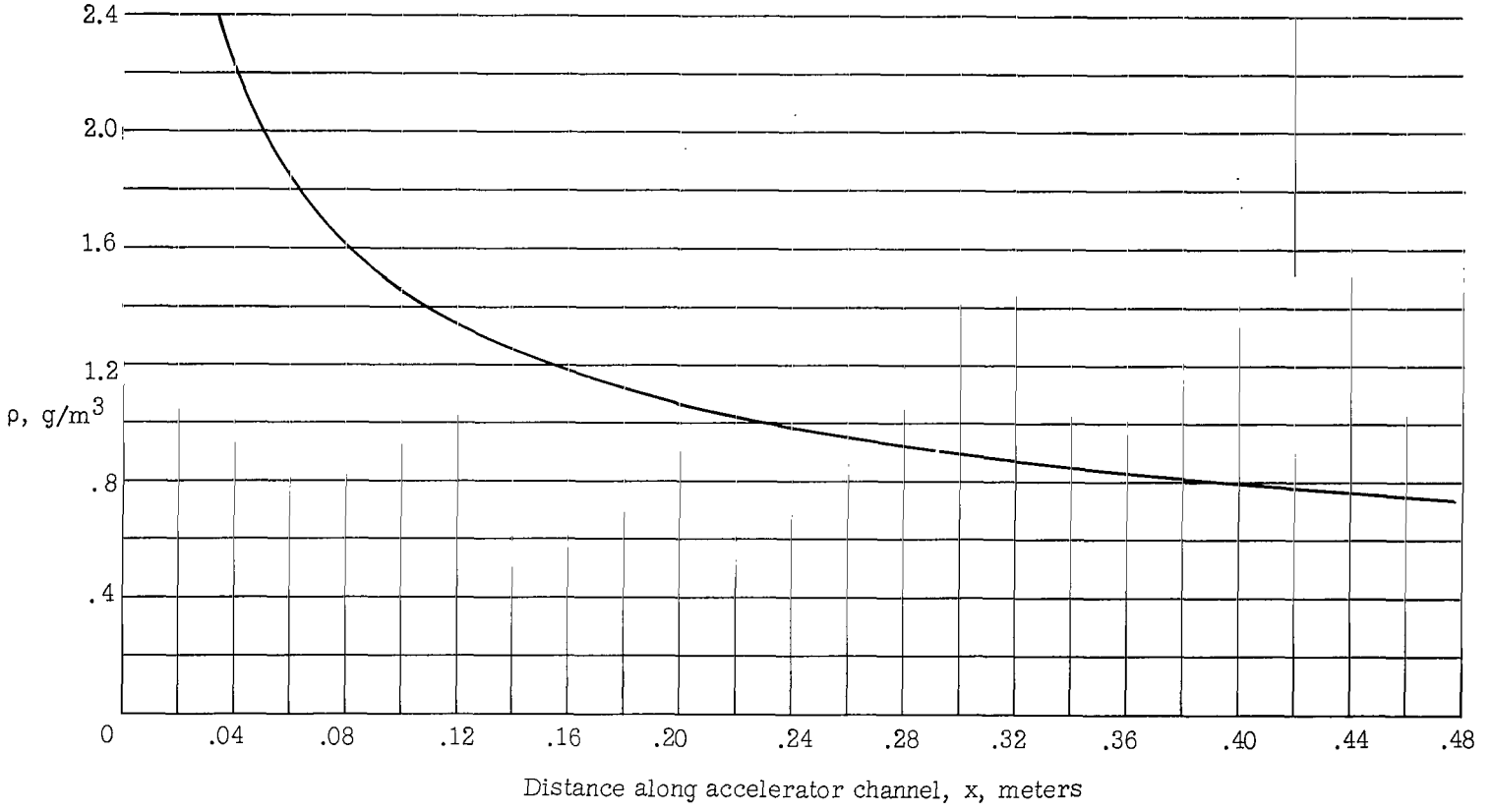

Figure 10.- Mass-density distribution.

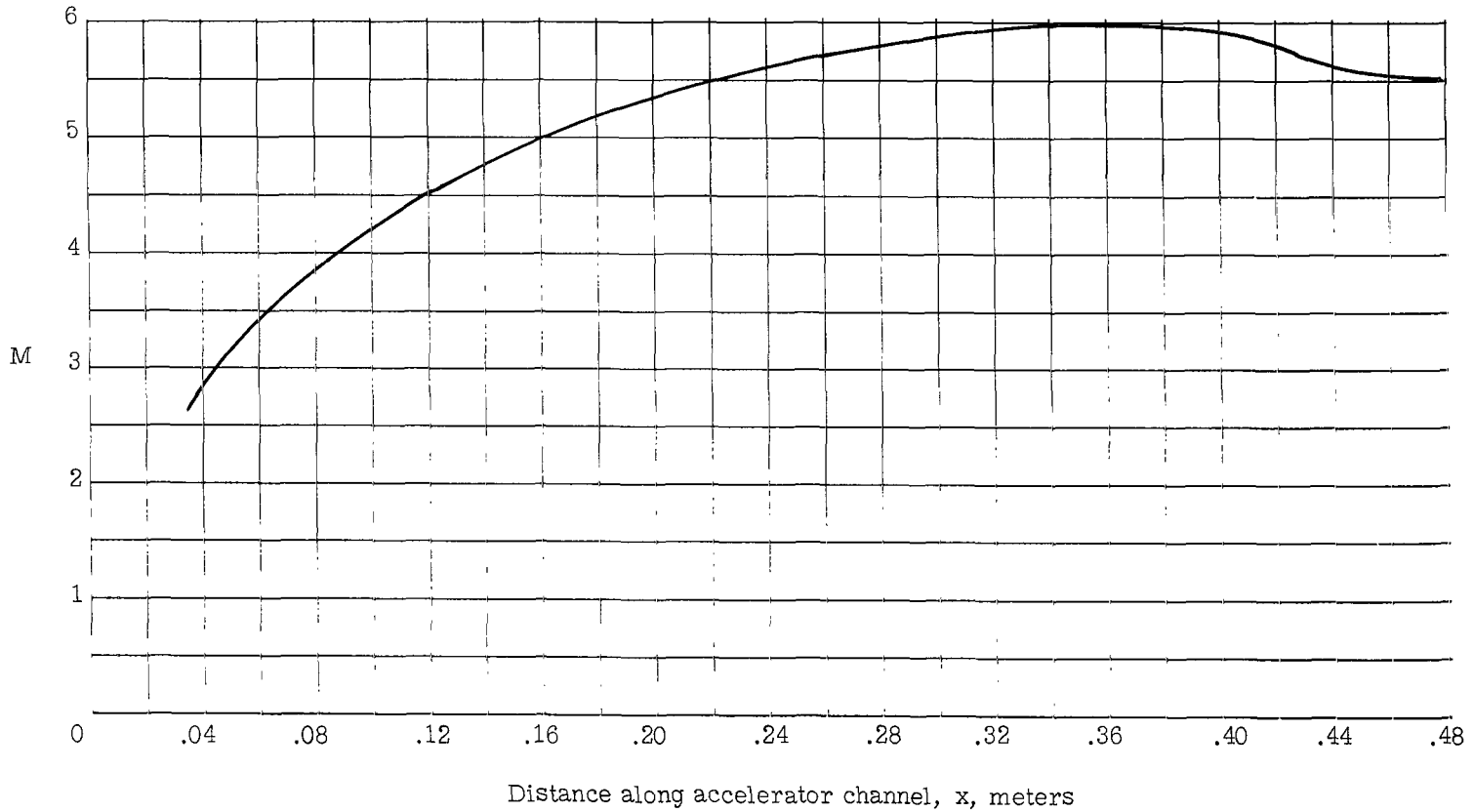

Figure 11.- Mach number distribution.

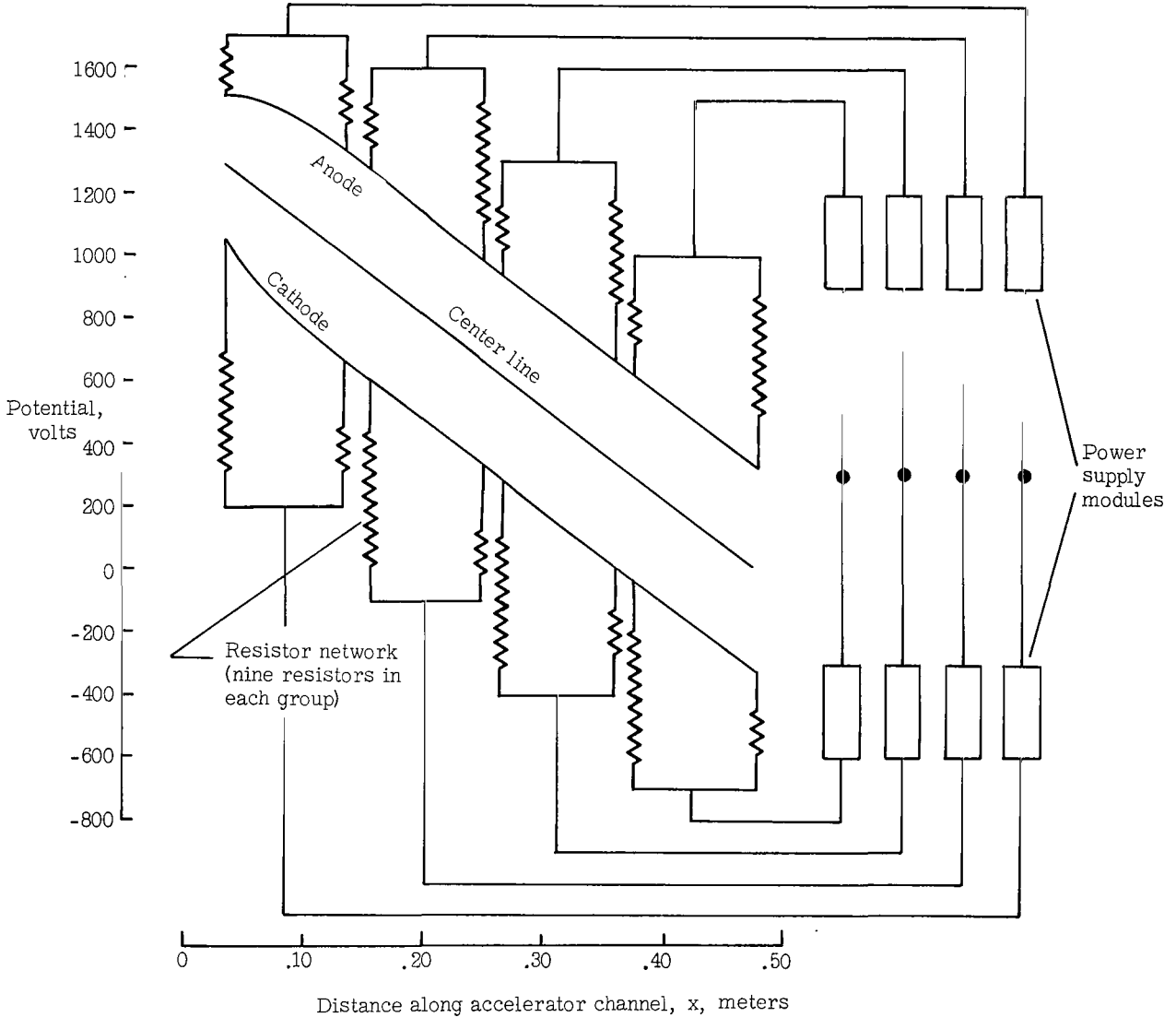

Figure 12.- Anode- and cathode-wall potential distributions, resistor network, and connections to power supply.

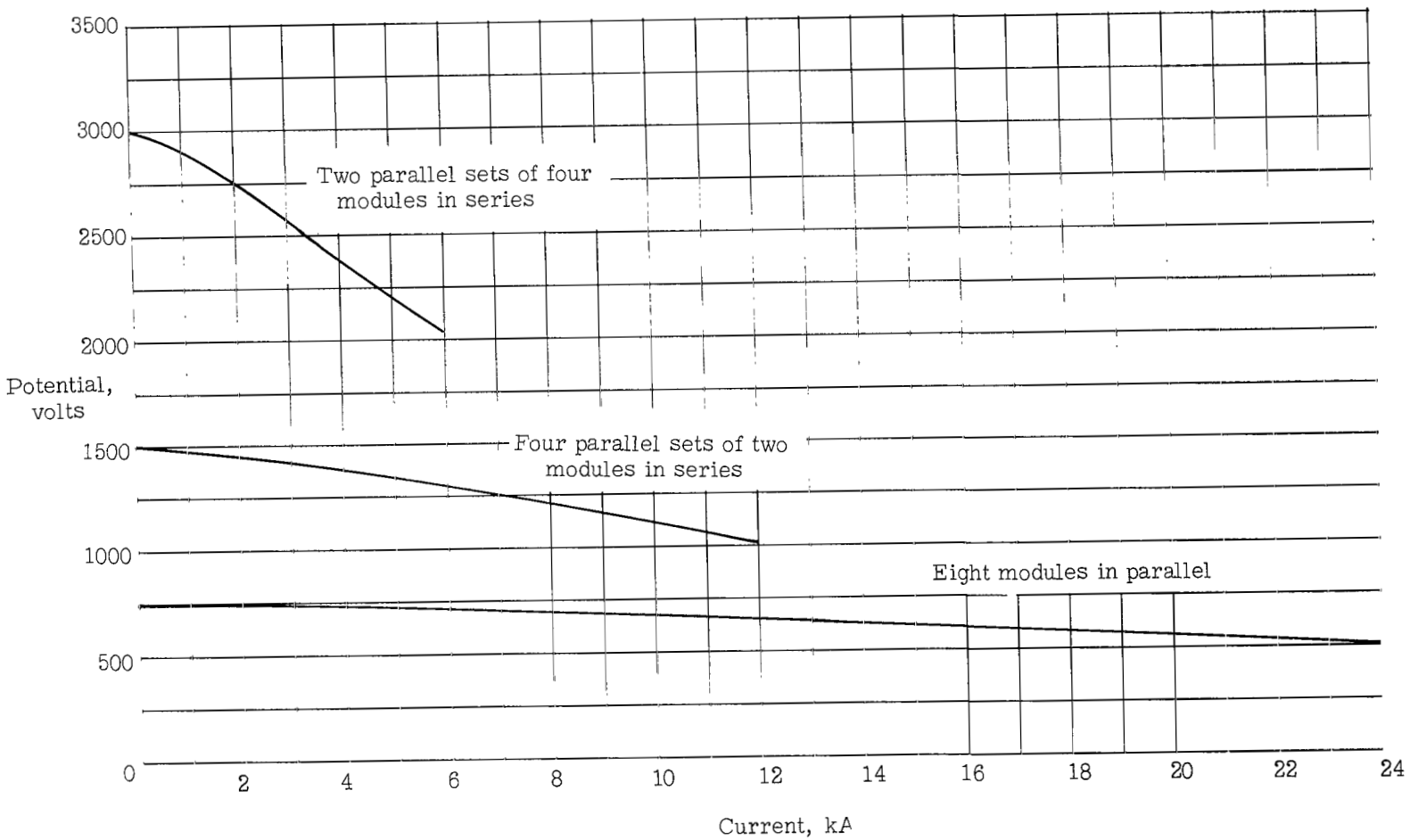

Figure 13.- Accelerator power-supply characteristics.

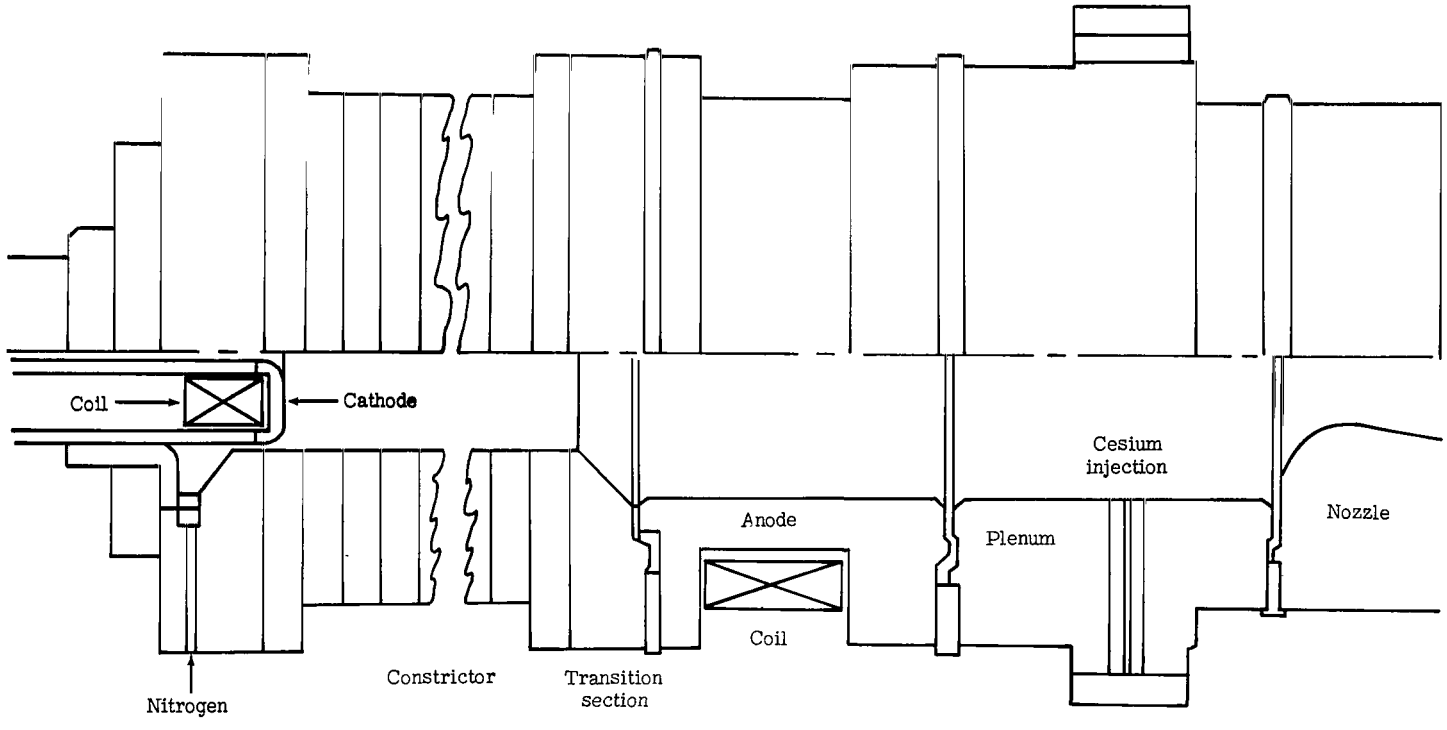

Figure 14.- Schematic diagram of arc heater.

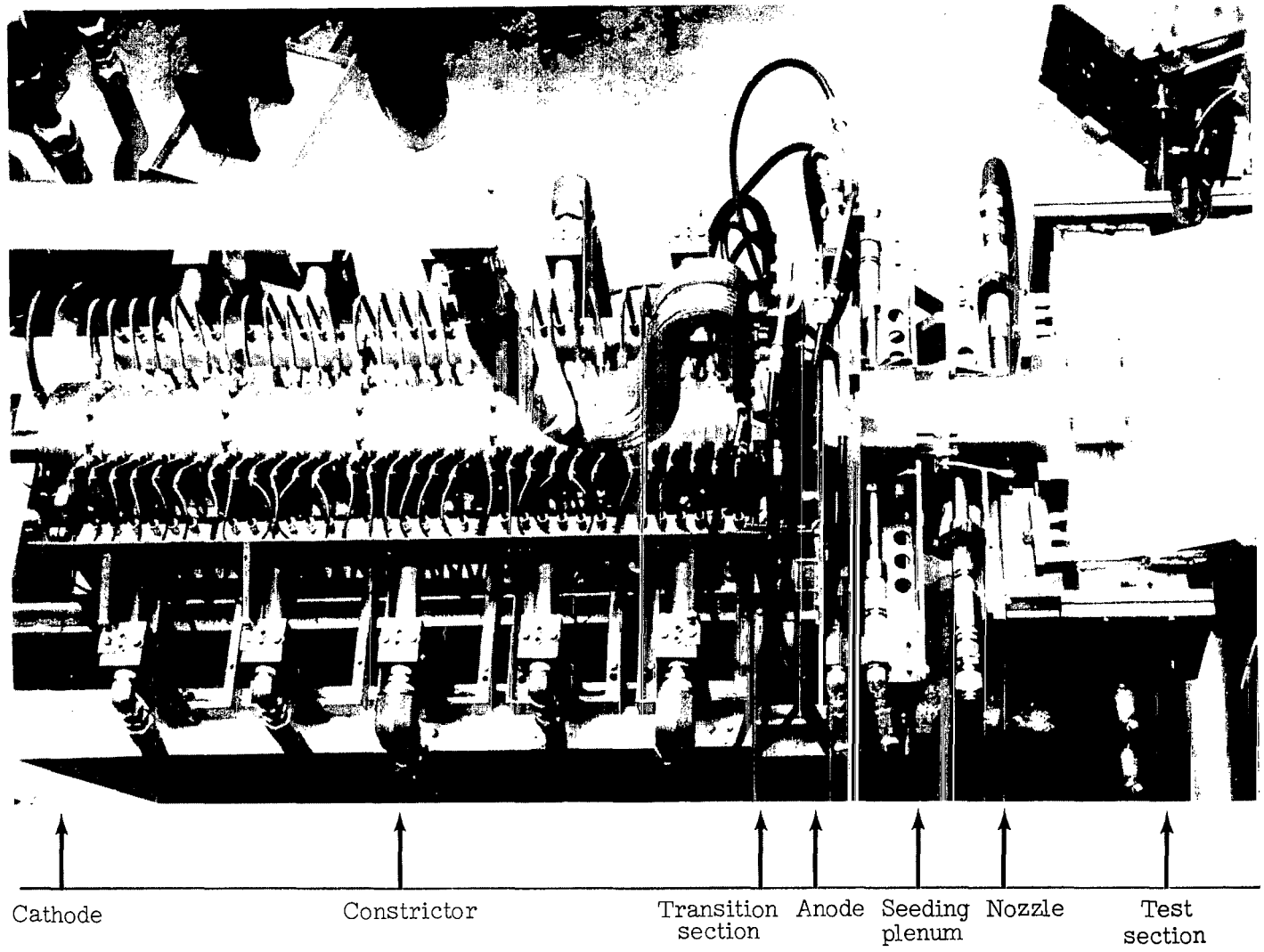

Figure 15.- Arc-heater plasma source (photograph taken from above).

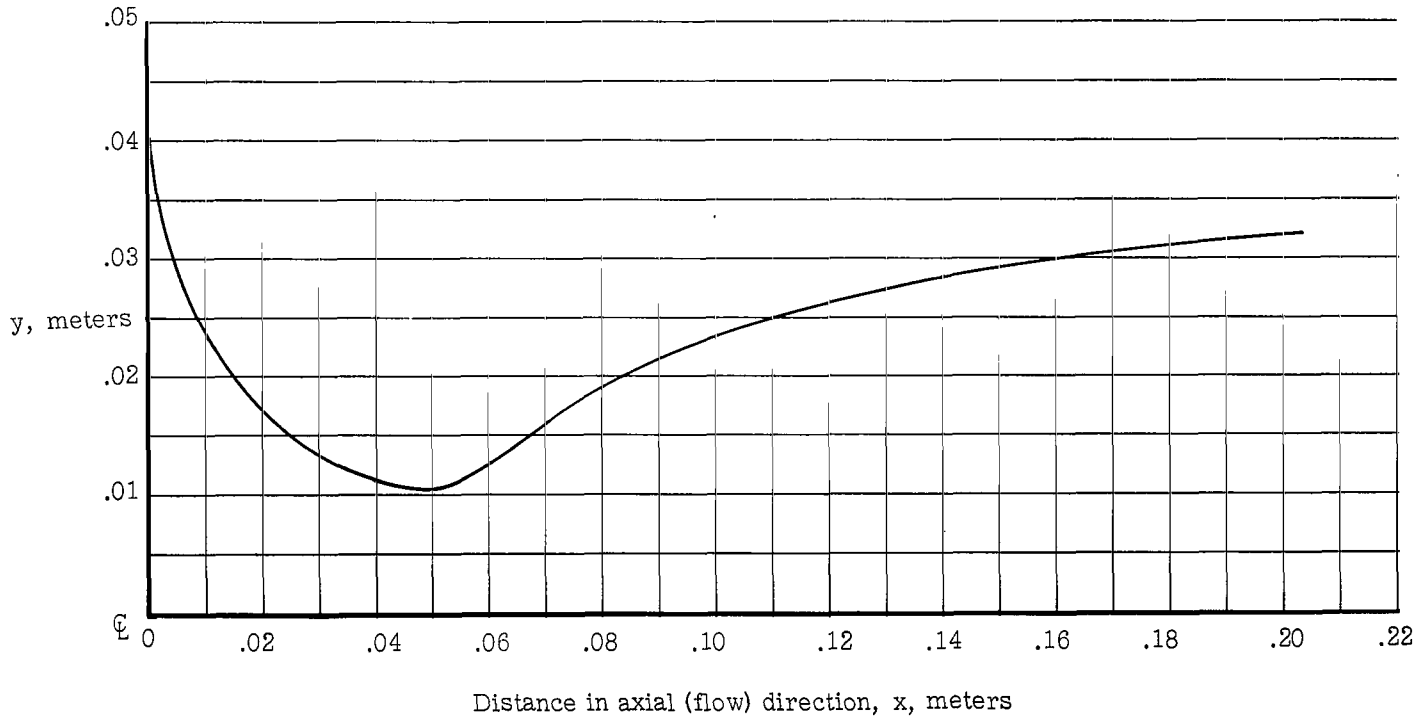

Figure 16.- Contour of supersonic nozzle.

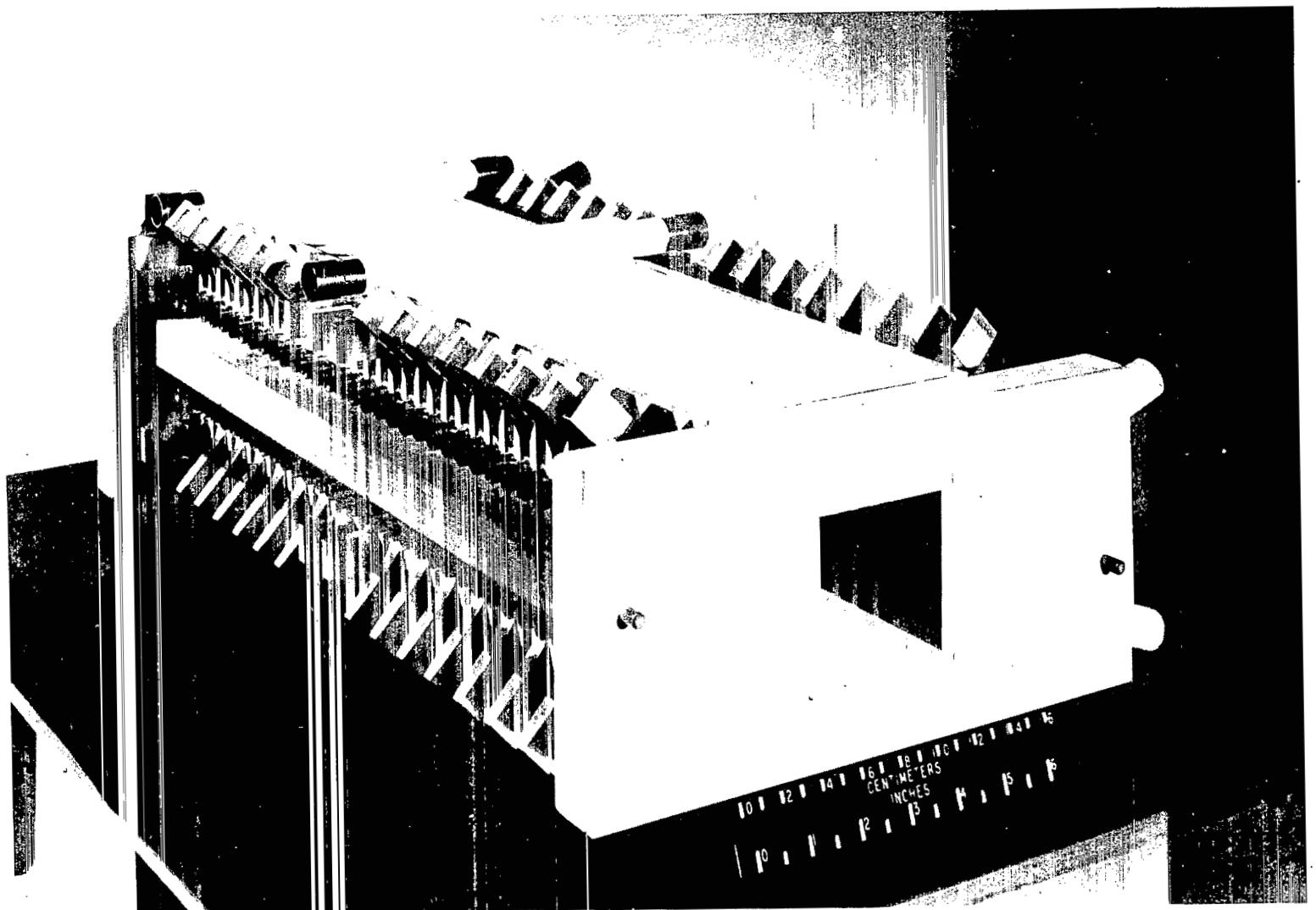

L-66-1913

Figure 19.- Assembled accelerator.

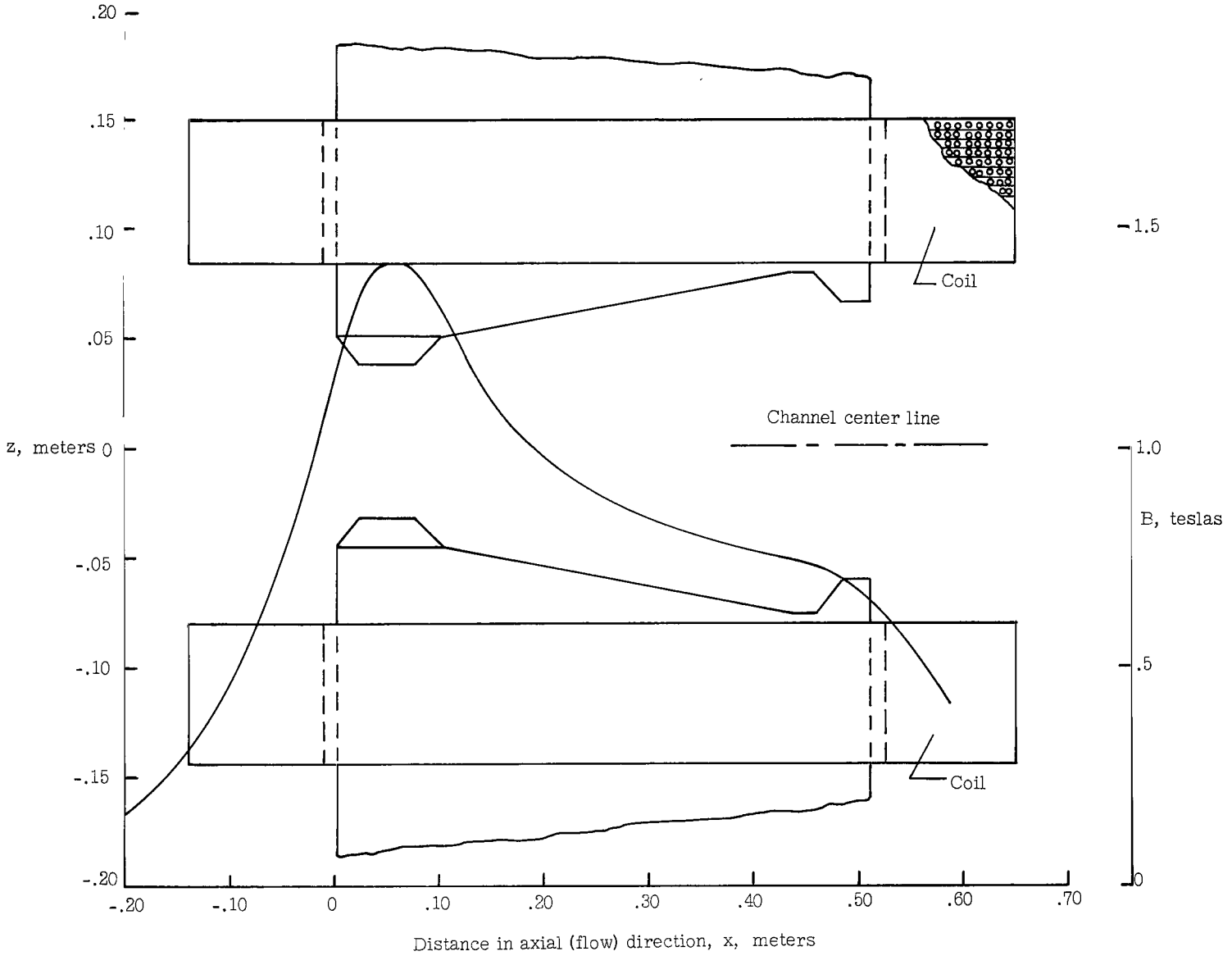

Figure 20.- Magnet pole contour and final distribution of magnetic flux density on center line.

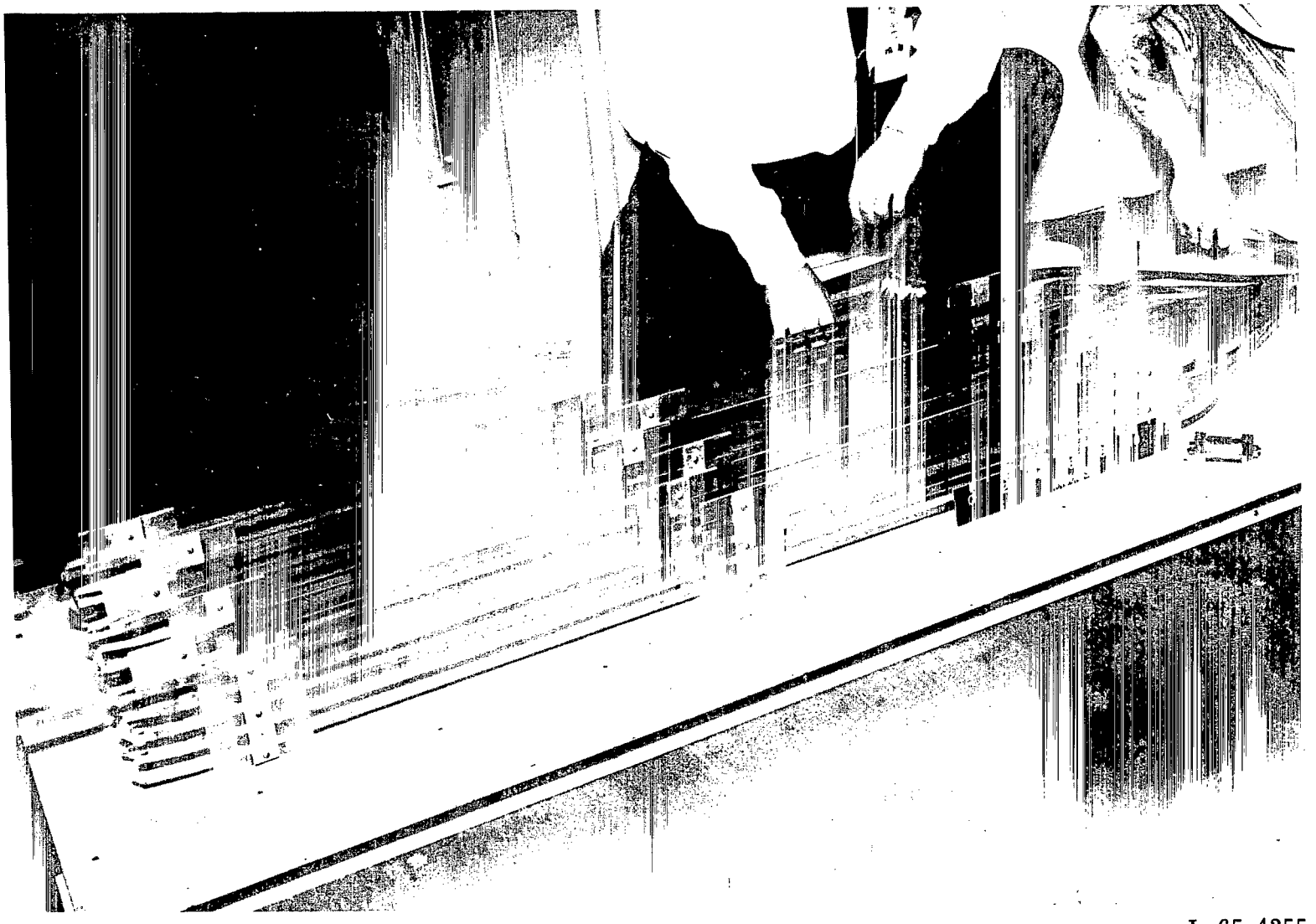

L-65-4255

Figure 21.- Working model of accelerator resistor.

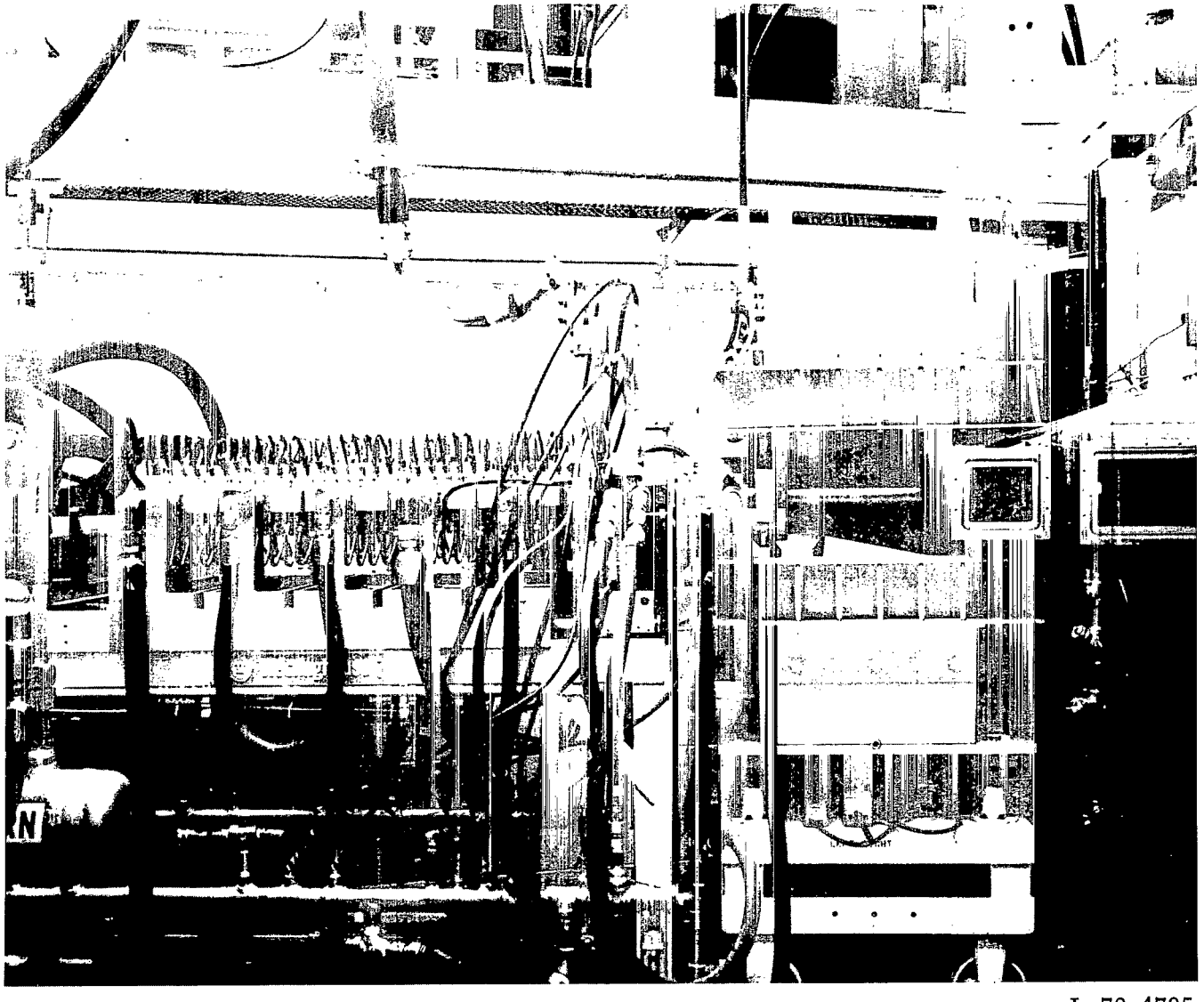

L-70-4795

Figure 22.- Arc heater, magnet, and test section.

"The aeronautical and space activities of the United States shall be conducted so as to contribute . . . to the expansion of human knowledge of phenomena in the atmosphere and space. The Administration shall provide for the widest practicable and appropriate dissemination of information concerning its activities and the results thereof."

— NATIONAL AERONAUTICS AND SPACE ACT OF 1958

NASA SCIENTIFIC AND TECHNICAL PUBLICATIONS

TECHNICAL REPORTS: Scientific and technical information considered important, complete, and a lasting contribution to existing knowledge.

TECHNICAL NOTES: Information less broad in scope but nevertheless of importance as a contribution to existing knowledge.

TECHNICAL MEMORANDUMS: Information receiving limited distribution because of preliminary data, security classification, or other reasons.

CONTRACTOR REPORTS: Scientific and technical information generated under a NASA contract or grant and considered an important contribution to existing knowledge.

TECHNICAL TRANSLATIONS: Information published in a foreign language considered to merit NASA distribution in English.

SPECIAL PUBLICATIONS: Information derived from or of value to NASA activities. Publications include conference proceedings, monographs, data compilations, handbooks, sourcebooks, and special bibliographies.

TECHNOLOGY UTILIZATION PUBLICATIONS: Information on technology used by NASA that may be of particular interest in commercial and other non-aerospace applications. Publications include Tech Briefs, Technology Utilization Reports and Technology Surveys.

Details on the availability of these publications may be obtained from:

SCIENTIFIC AND TECHNICAL INFORMATION OFFICE

NATIONAL AERONAUTICS AND SPACE ADMINISTRATION

Washington, D.C. 20546